Lead optimization and biological evaluation of fragment-based cN-II inhibitors

Rémi Guillon, Rahila Rahimova, Preeti Preeti, David Egron, Sonia Rouanet, Charles Dumontet, Nushin Aghajari, Lars Petter Jordheim, Laurent Chaloin, Suzanne Peyrottes

Lead optimization and biological evaluation of fragment-based cN-II inhibitors

Rémi Guillon[1], Rahila Rahimova[2], Preeti[3], David Egron[1], Sonia Rouanet[1], Charles Dumontet[4], Nushin Aghajari[3], Lars Petter Jordheim[4], Laurent Chaloin[,2] and Suzanne Peyrottes*[,1]*

[1] Institut des Biomolécules Max Mousseron (IBMM), UMR 5247 CNRS, Université de Montpellier, ENSCM, Campus Triolet, cc1705, Place Eugène Bataillon, 34095 Montpellier, France

[2] Institut de Recherche en Infectiologie de Montpellier (IRIM), CNRS, Université de Montpellier, 34293 Montpellier, France

[3] Molecular Microbiology and Structural Biochemistry, UMR5086 CNRS – Université Lyon 1, 7 Passage du Vercors, 69367 Lyon, France

[4] Université de Lyon, Université Claude Bernard Lyon 1, Centre de Recherche en Cancérologie de Lyon, INSERM U1052, CNRS UMR 5286, Centre Léon Bérard, 69008 Lyon, France

* shared *corresponding authorship*

Keywords: 5'-nucleotidase, enzyme inhibitor, cancer

ABSTRACT: The development of cytosolic 5'-nucleotidase II (cN-II) inhibitors is essential to validate cN-II as a potential target for the reversion of resistance to cytotoxic nucleoside analogues. We previously reported a fragment-based approach combined with molecular modelling, herein, the selected hit-fragments were used again in another computational approach based on the Ilib-diverse (a software enabling to build virtual molecule libraries through fragment based de novo design) program to generate a focused library of potential inhibitors. A molecular scaffold related to a previously identified compound was selected and led to a novel series of compounds. Ten out of nineteen derivatives showed 50 to 75% inhibition on the purified recombinant protein at 200 µM and among them three derivatives (**12, 13** and **18**) exhibited K_i in the sub-millimolar range (0.84, 2.4 and 0.58 mM, respectively). Despite their only modest potency, the cN-II inhibitors showed synergistic effects when used in combination with cytotoxic purine nucleoside analogues on cancer cells. Therefore, these derivatives represent a family of non-nucleos(t)idic cN-II inhibitors with potential usefulness to overcome cancer drug resistance especially in hematological malignancies in which cN-II activity has been described.

INTRODUCTION

5’-nucleotidases (EC 3.1.3.5) are a family of enzymes that catalyze the hydrolysis of 5’-nucleoside monophosphates (5’-nucleotides) into their corresponding parent nucleosides and inorganic phosphate, and thereby play a key role in the metabolism of nucleotides. The membrane-bound ecto-5’-nucleotidase, CD73, is mainly responsible for the conversion of extracellular adenosine 5’-monophopshate (AMP) into adenosine, whereas intracellular 5’-nucleotidases (cN-I, cN-II, cN-III, cdN, mdN) regulate the intracellular pools of both purine- and pyrimidine-based 5’-nucleotides and nucleosides, depending on their substrate specificity and intracellular compartments [1] [2]. cN-IA uses both AMP and pyrimidines and is expressed in muscles, whereas its homologue cN-IB is AMP specific and ubiquitously expressed. The cytosolic cN-II and cN-IIIA are GMP/IMP and pyrimidine preferring, respectively. cN-II is ubiquitously expressed and at a higher level in highly proliferating cells, whereas cN-IIIB is important in erythrocytes but has also been found in many other tissues. More recently, a cN-IIIB was described and found to be specific to 7-methyl-GMP [3]. Finally, the cytosolic cdN and the mitochondrial mdN are active on deoxyribonucleosides phosphorylated on 3’ or 5’, with a preference towards pyrimidine derivatives.

Several studies have shown that deficiencies of these proteins are associated to severe diseases. For example, deficiency in cN-III due to genetic mutations leads to hemolytic anemia [4], CD73 deficiency is associated to arterial calcification [5], and the *NT5C2* (coding for cN-II) containing locus has been associated with autosomal recessive spastic paraplegia and psychiatric disorders [6-8]. In addition, high expression level or activity of cN-II in tumor cells is associated with resistance to cytotoxic nucleoside analogues and nucleobases [9-11]. Its direct role in this resistance was shown by the sensitization of human cancer cells to purine nucleoside analogues after inhibition of its expression by shRNA [12]. Based on these observations, cN-II represents an attractive target to revert cancer resistance, and the use of cN-II inhibitors in combination with chemotherapy involving cytotoxic nucleosides may be of great interest.

Purine ribonucleoside analogues modified at the 5’-position were the first inhibitors of cN-II reported in the literature (Fig. 1) [13]. 5’-Deoxy-5'-isobutylthio derivatives of adenosine and inosine inhibited 50% of the nucleotidase activity (extracted from rat liver) at 2-10 mM. Recently, it was shown that fludarabine was able to interfere with human cN-II as a mixed-inhibitor (K_i 0.5 mM and K_i' 9 mM) [14]. Over the last decade, we have also identified, developed and studied cN-II inhibitors by using virtual screening [15], a substrate analogue-based approach [16-18], and finally a fragment-based drug discovery (FBDD) strategy [19]. All these derivatives behaved as weak to modest cN-II inhibitors with K_i in the millimolar range (Fig. 1). Since these compounds act as competitive

inhibitors and taking into account that cN-II is also named high-K_M 5'-nucleotidase, it is not surprising to observe such high K_i values (K_M for inosine 5'-monophosphate (IMP) is ~ 0.5 mM). Despite this, co-exposure of cancer cells to nucleoside analogues and some of these cN-II inhibitors potentiated the effect of cytotoxic nucleoside analogues [14, 15].

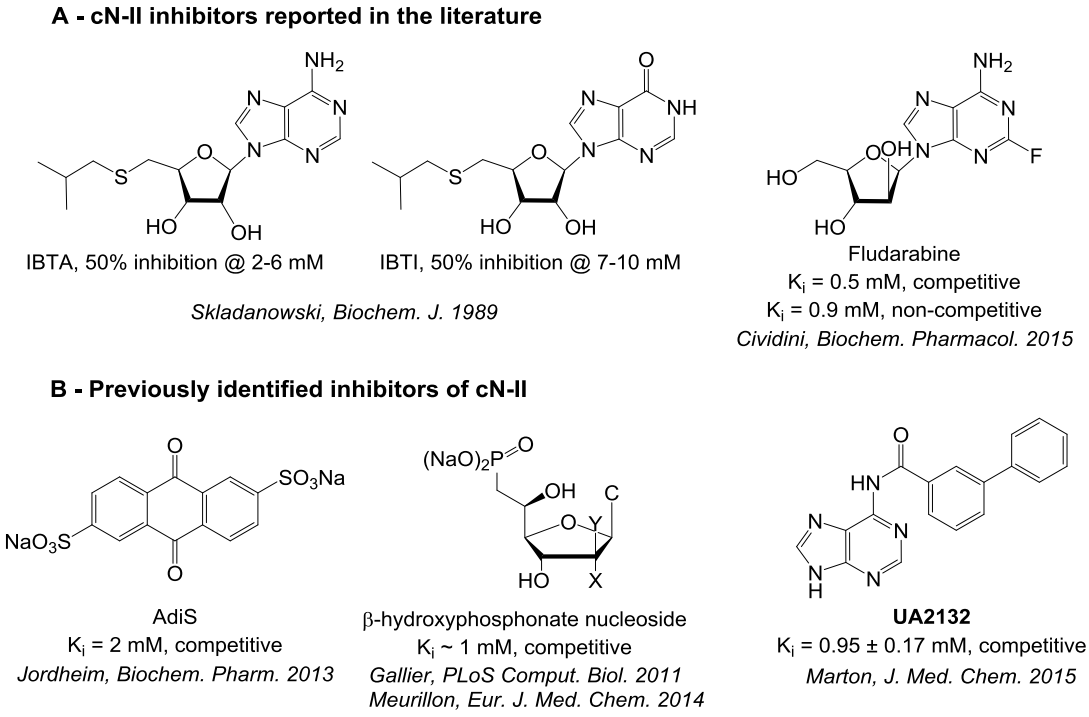

Figure 1. Chemical structures of the cN-II inhibitors reported in the literature. IBTA: 5'-Isobutyl thioadenosine; IBTI: 5'-Isobutylthioinosine; AdiS: Anthraquinone-2,6-disulfonic acid, disodium salt; C: cytosine; Y=H and X=OH, or Y=OH and X=H.

Herein, we pursue the development of cN-II inhibitors using a small set of fragment hits, which have been previously selected by a FBDD approach [19], to build up a virtual library. The latter was generated using the Ilib-diverse software (http://www.inteligand.com), and involved the random association of various fragments and chemical groups in order to enhance binding affinity and/or retain drug-like properties such as water solubility. These *in silico* approaches have been successfully applied to the design of potential lead compounds such as creatine kinase [20] and phospholipase [21] inhibitors. *In silico* virtual screening was performed on the basis of experimental cN-II crystal structures [22] and compounds with the most favorable docking scores were carefully analyzed. Thus, one derivative was hand-picked to guide structural optimization, on the basis of its resemblance with a previously identified inhibitor.

RESULTS AND DISCUSSION

***In silico* drug design, library generation and selection process.** We combined *in silico* drug design approaches including virtual library generation followed by *in silico* screening by molecular docking to identify potential inhibitors [23, 24]. Briefly, virtual flasks containing the most active fragments previously identified by nuclear magnetic resonance (NMR) screening and measurement of the inhibition of the enzyme activity *in vitro* [19], were used for the combinatorial generation of novel chemical scaffolds. An overview of the process is presented in Figure 2. Flask 1 contained 21 fragments, whereas flasks 2 and 3 contained 15 fragments each (structures of the components are listed in table S1 and mainly include aromatic and bicyclic derivatives, nitrogen-containing heterocycles such as benzimidazoles, purines…). Finally, flask 4 contained 43 polar or ionisable building blocks (alcohols, carboxylic acids, phosphoesters…, see Table S1) available from the Ilib-diverse software.

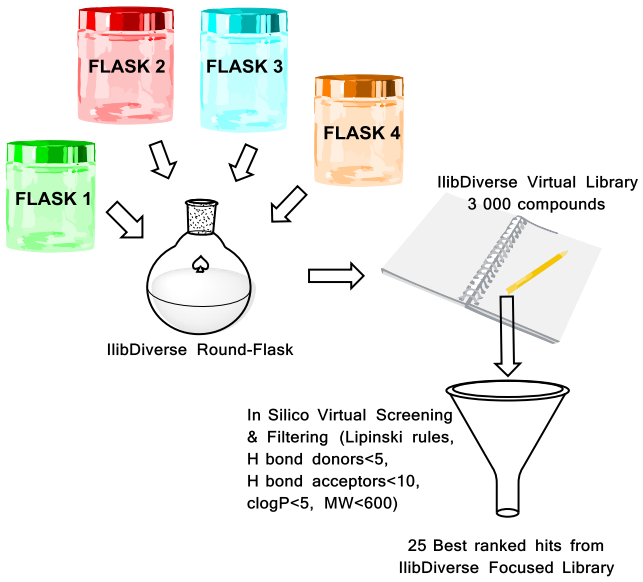

Figure 2. Schematic view of the focused library generation. Virtual flasks 1, 2 and 3 contain hit fragments previously identified as cN-II binders by NMR. Combination of one fragment from each flask with an additional functional polar group (flask 4) is achieved *in silico* using the Ilib-diverse software and leading to a virtual library of 3,000 compounds. All obtained compounds were evaluated for their theoretical binding affinity by docking on cN-II crystal structure.

The Ilib-diverse tool generated a focused virtual library by using a Monte-Carlo-based random fragment connection including general rules of chemical synthesis feasibility. During this process, the software is randomly selecting fragments from each flask and generates molecules with a broad molecular diversity. In our setup, we defined a higher importance for experimentally validated hit fragments (cN-II binders identified by NMR) meaning that the frequency of insertion of these

fragments in the final library will be higher compared to the low-active fragments (underlined fragments in Table S1). To further increase the diversity and also to improve the aqueous solubility of compounds, combination of one fragment taken from each of the three flasks was followed by the addition of a fourth ionisable chemical group (building blocks already included in the program that can be also considered as a fourth flask). Thus, a total of 3,000 compounds was generated (Ilib-diverse virtual library), all meeting the criteria of orally-delivered drug like compounds according to Lipinski's rule of five (one exception was the molecular weight with an upper limit at 600 Da instead of 500 Da). Then, all compounds were evaluated by molecular docking on cN-II. The ones showing a lower score than that of our previously identified lead compound (Fig. 1, **UA2132**) and hitherto most potent cN-II inhibitor reported were discarded, leaving a total of 884 compounds for further consideration. To narrow the number of molecules to be further examined for synthetic accessibility, we focused on compounds with highest docking scores (using a cut-off value of 125, which is approximately 20 points above the docking score of **UA2132**) resulting in a selection of 25 chemical structures (Table S2).

The analysis of structure similarity and fragments composition of these 25 selected hits indicates that some skeletons were privileged during the library generation and filtering process. Indeed, numerous assemblies consisting of polycyclic aromatic structures linked to a phenyl or biphenyl fragment were found to promote a favorable binding according to the docking results. Among these, one derivative particularly attracted our attention (Fig. 3B, **Ilib-72**) due to its structural similarity with the previously identified cN-II inhibitor **UA2132** (Fig. 3A). In addition, several hit compounds with docking scores being slightly lower than our cut-off value (125) were identified as structural analogues of **UA2132** or at least holding an adenine moiety linked to an aromatic cycle through an amide link (see Table S2, hits highlighted in bold characters). Therefore, instead of performing the chemical synthesis of all 25 best-ranked hit compounds, we prioritized the structure optimization of our lead compound considering the structural variations observed in **Ilib-72** as it was the best-ranked analogue of **UA2132**.

In this respect, molecular docking studies were performed to predict and compare the potential binding modes of **Ilib-72** with **UA2132**.

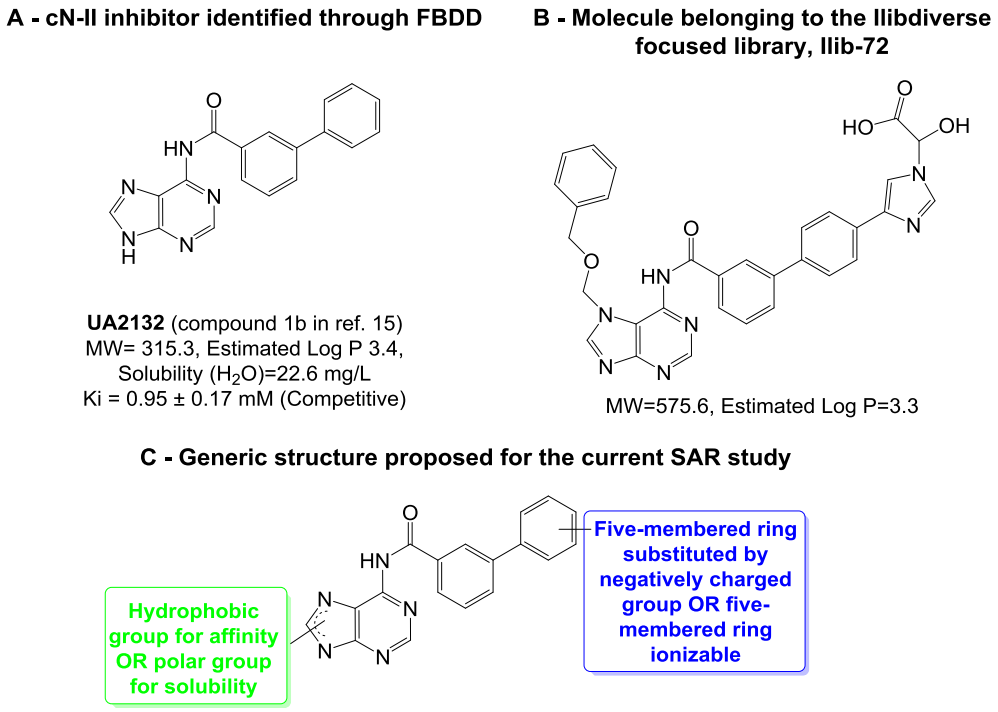

Figure 3. Chemical structures of the potential cN-II inhibitors. (A) Previously identified derivative **UA2132** with inhibition mode and constant; (B) Hand-picked derivative (**Ilib-72**) from the focused library; (C) Generic structure proposed for structural optimization.

Since **UA2132** is a competitive inhibitor, the docking of hit compounds was achieved in the substrate binding site (Fig. 4). One should note that the crystal structure used for modelling (PDB 2XCW) was an inactive mutant in which one of the catalytic residues D52 was mutated to N. Compared to other crystal structures, this mutation does not change the coordination of Mg^{2+} ion (hexa-coordinated with D/N52, D54, D351, 2 water molecules and one phosphate oxygen from IMP). This mutation was used by Wallden and colleagues in order to prevent substrate hydrolysis during crystallization, thereby giving an image of the position of the substrate [25]. Similar docking poses have been obtained using the wild-type enzyme (2JC9). For **UA2132**, the prediction suggests only one binding mode with the adenine moiety near the catalytic residues which interact with the magnesium ion (the two first *via* coordination bonds and the latter *via* a water molecule). In contrast to **UA2132**, two binding orientations were predicted for **Ilib-72** (Fig. 4A & 4B) with comparable docking scores (126.9 and 126.1). The most favorable binding mode is shown in Figure 4A with the purine and the benzyloxymethyl group near the magnesium ion. However, in the second binding mode the α-hydroxyacetic acid chain is chelating the magnesium ion within a more compressed structure (Fig. 4B). This latter may reflect the real binding orientation of this compound since the

natural substrate (IMP) also carries a negative charge on the phosphate oxygen. Interestingly, **Ilib-72** occupies a large space which extends beyond the substrate binding cavity (Fig. 4C).

Based on this docking information, we decided to keep the *N-6* biaryl substituted adenine skeleton (present in **UA2132**) and to add various groups either on the *N-7* or *N-9* position of the purine, and/or a five-membered nitrogen containing heterocycle on the biaryl moiety (Fig. 3C and 5). Both substituents were chosen for their ability to either increase affinity and/or improve solubility of the final derivatives. Indeed, under physiological conditions tetrazole and phosphonate groups would be partially or completely protonated (Fig. 5).

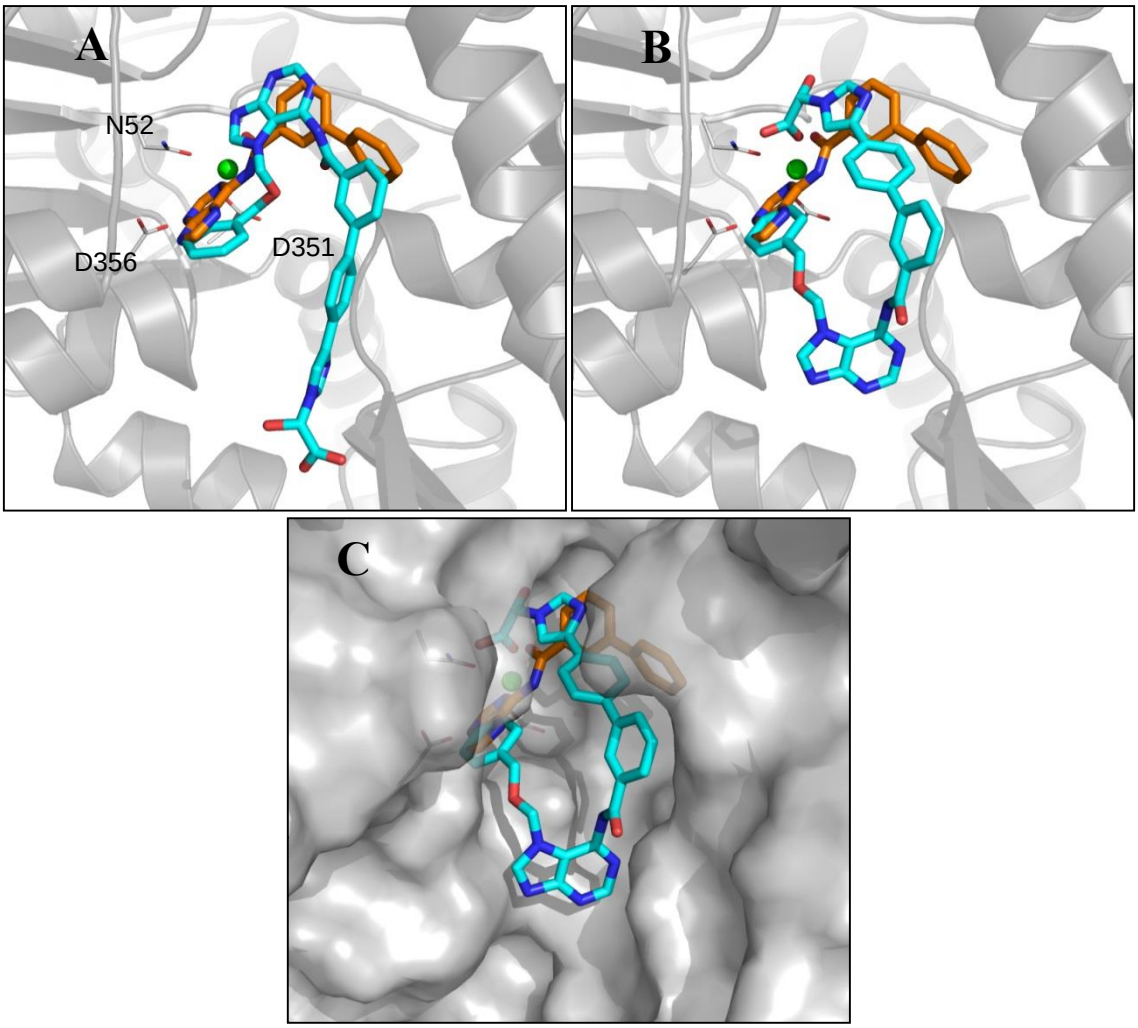

Figure 4. A) Preferential binding mode predicted by molecular docking for **UA2132** (orange sticks) and **Ilib-72** (cyan sticks). **B**) Second binding mode identified for **Ilib-72** showing an inversed orientation allowing the ionic interaction between carboxylic group and magnesium ion (depicted as a green sphere). **C**) Same docking as in panel (B) with cN-II in surface representation to appreciate the substrate binding site. Catalytic residues are shown in grey thin sticks.

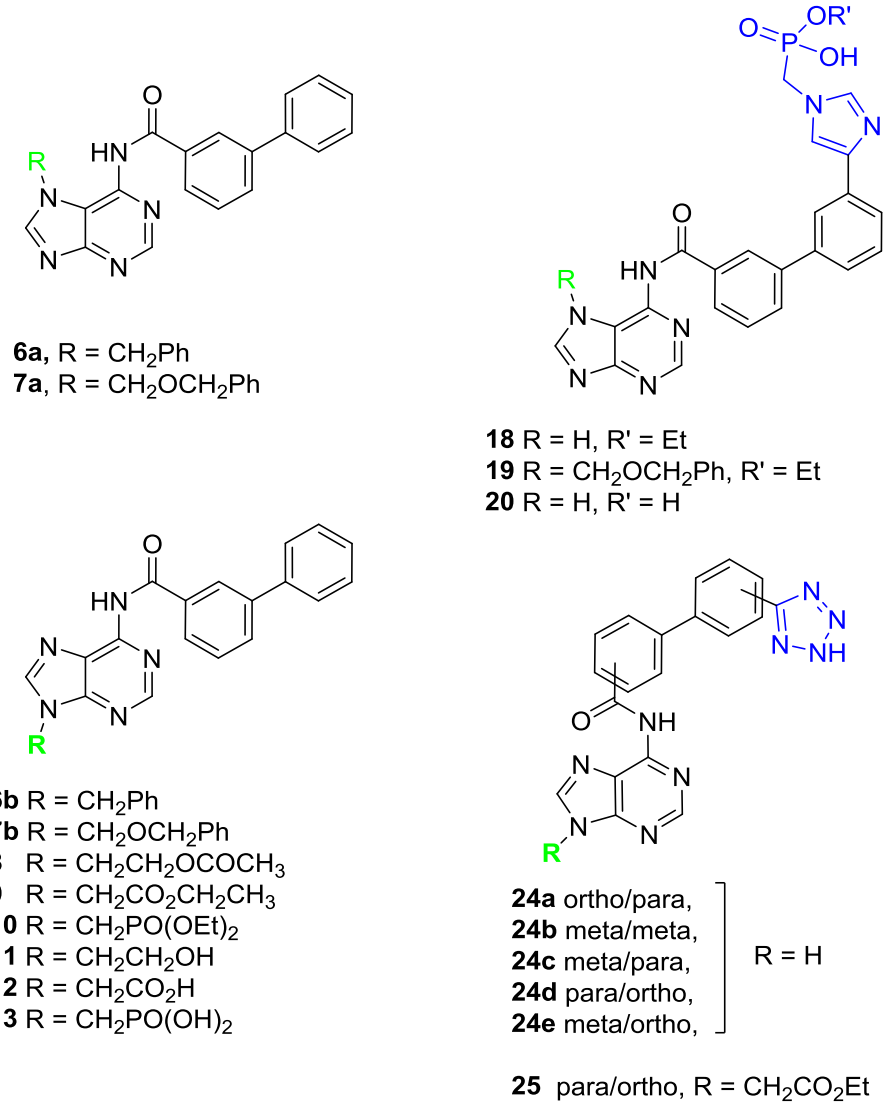

Figure 5. Structures of the studied compounds **6-13**, **18-20**, **24a-e** and **25**.

Synthesis. The targeted compounds, presented in Figure 5, may be divided into three groups corresponding to: (i) *N*-7 or *N*-9 substituted derivatives of **UA2132** (**6-13**), (ii) Ilib-72 analogues incorporating a polar substituent on the imidazole ring (**18-20**) and (iii) analogues incorporating a tetrazole ring as ionisable five-membered ring (**24-25**).

First, different substitutions on positions *N*-7 or *N*-9 of the purine heterocycle (Fig. 5) were envisaged: (i) a hydroxyethyl chain (**8** and **11**), a methyl phosphonate (**10** and **13**) or a methylcarboxylate (**9** and **12**) in order to improve the aqueous solubility of **UA2132** as this was identified as a limit for its *in vivo* evaluation (unpublished data); (ii) a benzyl (**6a-b**) or a benzyloxymethyl (**7a-b**) as observed within the structure of **Ilib-72** for better affinity to the target protein. Then, due to synthetic issues we envisaged, as the closest analogues of **Ilib-72**, the replacement of the α-hydroxyacetic acid chain by non-classical bio-isosteres such as a methyl

phosphonate group (compounds **18**, **19** and **20**) mimicking the acetate anion and being partially ionized at physiological pH. Another modification consisted in the replacement of both the imidazole ring and the α-hydroxyacetic acid chain by a tetrazole ring (compounds **24a-e**). Indeed, tetrazole is known to present similar physicochemical properties as a carboxyl group, and it is increasingly used in drug development. Furthermore, tetrazole can exist in both neutral and anionic states. The latter would allow the formation of salts that may be valuable for water solubility.

The general synthetic approach used to prepare new bi-aryl carboxamide derivatives of adenine incorporating various *N-7*/*N-9*-substituants (**6-13**), *N*-methylphosphonate and imidazole moieties (**18-20**) or *C*-branched tetrazole (**24a-e** and **25**) consists of coupling adenine or *N-7*/*N-9*-substituted adenine (**1-5**) with commercially available biphenyl carbonyl chlorides (Scheme 1) or substituted biphenyl carboxylic acids (**17, 23a-e**) (Schemes 2 and 3). When using carboxylic acids, an excess of the activation reagent, *N*,*N'*-carbonyldiimidazole (CDI), was required as well as a catalytic amount of 4-dimethylaminopyridine (DMAP), and the coupling reaction was performed in anhydrous dimethylformamide (DMF) at 100 °C until starting material was consumed (HPLC monitoring). In addition, due to the limited thermal stability of DMF at elevated temperature (leading to side reactions such as dimethyl amination and/or formylation), DMF was replaced by *N*-methylpyrrolidinone (NMP) for prolonged reaction time at temperatures over 100 °C. In a few cases, low yields were observed for this coupling step and were associated to the fact that chromatographic separation of the starting material and the desired compound was difficult. In addition, chemical instability was observed for compound **7a**, which was only obtained in 81.8% purity.

Alkylation reactions (Scheme 1) were carried out by reacting adenine with the appropriate commercially available alkyl halide in DMF, using potassium carbonate as base. When using benzyl bromide or benzylchloromethyl bromide, formation of both *N-7*/*N-9*-regioisomers (compounds **1a-b** and **2a-b**) was observed and they were separated by silica gel chromatography. The *N-7*-derivatives **1a** and **2a** were obtained in 20 and 43% yield, respectively. The regioselectivity of alkylation was unequivocally assigned by ^{1}HNMR and UV spectra. In DMSO-d_6, pronounced downfield shifts were observed for the signals corresponding to the H-8 and NH_2 of *N-7* when compared with those of *N-9* regioisomers. UV absorption spectra of *N-7* isomers showed slight bathochromic shifts (2-3 nm) compared to *N*-9 regioisomers. All these data are in agreement with data from the literature and corresponding to similar *N-7* and *N-9* purine isomers [26, 27].

The synthesis of *N*-(phosphonomethyl) derivatives **5** (scheme 1 for *N-9* adenine substitution) or **15** (scheme 2 for *N-1*-imidazole substitution) was performed employing diethyl *p*-toluenesulfonyloxymethylphosphonate as required alkylating reagent [28].

Scheme 1. Synthesis of *N-7* or *N-9* substituted derivatives of **UA2132**.

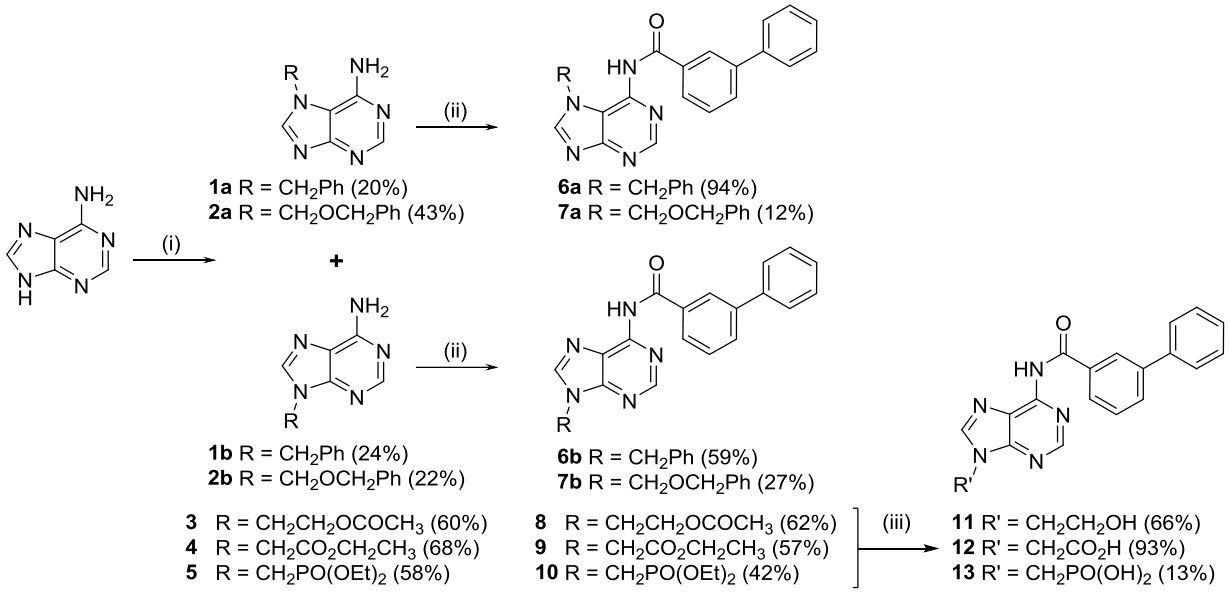

Reagents and conditions: (i) K_2CO_3, benzyl bromide (for **1a-b**) or benzylchloromethyl ether (for **2a-b**) or 2-bromoethylacetate (for **3**) or ethyl-2-bromoacetate (for **4**), DMF, rt, 1-48 h or NaH, diethyl p-toluenesulfonyloxymethylphosphonate (for **5**), DMF, 50 °C, 17 h; (ii) biphenyl-3-carbonyl chloride, pyridine, rt or 100 °C, 1-4 h. (iii) NaOH 2M, MeOH, 0 °C, 30 min (for **11** and **12**) or trimethylsilyl bromide (TMSBr), DMF, rt, 48 h (for **13**).

Cleavage of the phosphonate diethyl ether groups in the final step of synthesis of compounds **13** (scheme 1) and **20** (scheme 2) was carried out using trimethylsilyl bromine (TMSBr) and the desired compounds were obtained as their corresponding phosphonic acids following purification on C_{18} reverse phase and eventually cation-exchange chromatography to isolate them as sodium salts. One should notice that during the saponification of compound **16** (Scheme 2), concomitant loss of one ethyl group occurred and led to the phosphonate monoethyl derivative **17**. Moreover, attempts to obtain *N*-imidazolylmethylphosphonate derivative **19** incorporating a benzyloxymethyl group (BOM) on the *N-7* position of adenine was tedious (yield 6%) due to a relative instability of the BOM group.

For the series of compounds containing a tetrazole ring (compounds **24a-e** and **25**, scheme 3), intermediates **22a-e** have been prepared by 1,3-dipolar cycloaddition of nitrile precursors (**21a-e**) with sodium azide and trimethylamine hydrochloride in NMP. The cyano-substituted biphenyl esters **21a-e** were obtained beforehand according to the previously described Suzuki cross-coupling protocol [19] using commercially available starting materials such as 2-, 3- or 4-bromobenzonitrile

and 2-, 3- or 4-ethoxycarbonylbenzeneboronic acids. For compounds **24a**, **24d**, and **25**, the coupling reaction with the adenine moiety did not go to completion and low yields may be attributed to the steric hindrance associated to the ortho orientation of the substituents.

Scheme 2. Synthesis of Ilib-72 analogues incorporating a polar substituent on the imidazole ring.

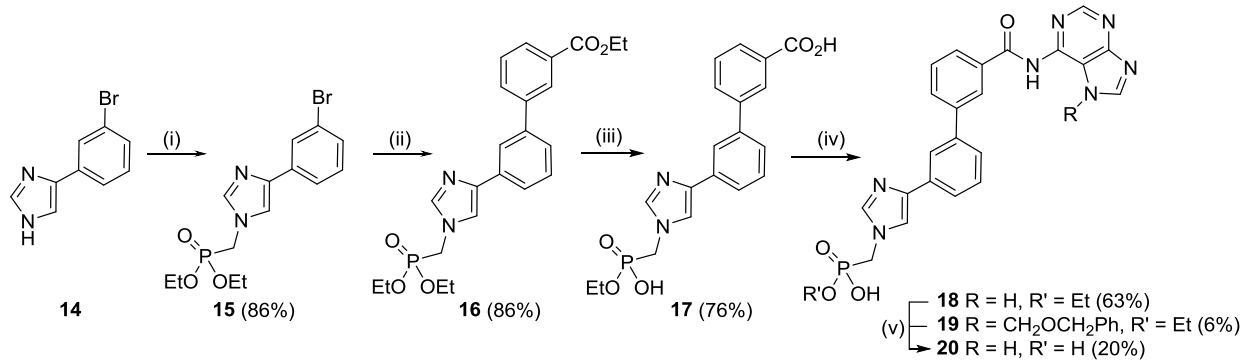

Reagents and conditions: (i) NaH, *p*-toluenesulfonyloxymethylphosphonate, DMF, 80 °C, 18 h; (ii) 3-ethoxycarbonylbenzeneboronic acid, $Pd(PPh_3)_4$, K_2CO_3, DMF, 100 °C; (iii) NaOH 2 M, EtOH, 1,4-dioxane, 80 °C. (iv) CDI, DMAP, adenine (for **18**) or **2a** (for **19**), DMF, 100 °C. (v) TMSBr, DMF, rt.

Scheme 3. Synthesis of derivatives incorporating a tetrazole ring.

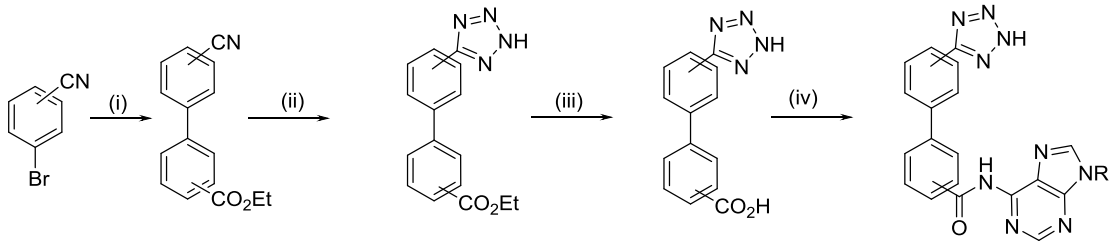

Reagents and conditions: (i) 2-, 3- or 4-ethoxycarbonylbenzeneboronic acid, $Pd(PPh_3)_4$, K_2CO_3, DMF, 100 °C; (ii) NaN_3, NEt_3.HCl, NMP, 150 °C (iii) NaOH 2 M, EtOH, 1,4-dioxane, 50 °C; (iv) CDI, DMAP, adenine or **4** or **5**, DMF or NMP, 80-150 °C.

Enzymatic studies. All synthesized compounds were evaluated for their inhibitory effect against recombinant cN-II using the malachite green-based assay with quantification of inorganic phosphate

produced from IMP (Tables 1-3) and the cLogP were calculated in order to estimate the impact of the various modifications on aqueous solubility, in comparison to **UA2132** used as a reference.

When introducing modifications in the *N-7* position (Table 1), no real improvement of the inhibitory effect could be observed (**1a**, **2a**, **6a**, **6b**, and **7a**) as compared to **UA2132**. An equivalent inhibition was observed at 200 µM for derivatives **6a** and **7a** which were substituted at the *N-7* position either by a benzyl or benzyloxymethyl group. This may be explained by a different orientation adopted by these derivatives in the binding site when compared to the compounds with *N-9* modifications. Substitutions on the *N-9* position of the purine heterocycle by aromatic substituents was found to reduce the activity of several compounds (**6b** and **7b**), whereas small and linear substituents (ethyl chain for **8** and **11** or methylcarboxylate **9** and **12**, or methylphosphonate **10** and **13**) increased the inhibition of the enzyme. Indeed, for the best inhibitors in this series (>60% at 200 µM) substitutions were including a carboxylic (**12**) or a phosphonate (**13**) group, especially when the negative charge was unmasked. Indeed, the presence of a carboxylate or a phosphonate group is expected to increase the overall aqueous solubility as anticipated (cf. cLogP). The presence of a biphenyl moiety was mandatory for the inhibition since smaller compounds lacking this group were almost- or fully inactive (**1b**, **2b**, and **3**).

In addition, substitution of the biphenyl moiety by a five-membered ring seems to play a major role as shown by the derivative **18** incorporating an imidazole and a (monoethyl)-methylphosphonate group (without any modification in *N-7* or *N-9,* derivative **19** was less efficient than **18**). Surprisingly, the fully unprotected compound **20** (with the closest similarity with **Ilib-72**) did not inhibit cN-II activity suggesting that the negative charges affect the binding mode of this compound (Table 2). According to the enzymatic inhibition, compound **18** appeared more advantageous (75% at 200 µM) and this may be explained by the partial negative charge compared to a fully charged compound **20** (harboring a double negative charge).

Table 1. Data for *N*-7 and *N*-9-substituted analogues of **UA2132**.

Compound	Structure	*N-7* / *N-9* substituent	**cLogP***	Inhibition (%) at 200 µM (or 1 mM when no inhibition at 200 µM) K_i (mM)
2132**	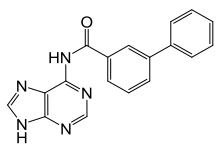	**none**	**3.4**	**68 ± 5%** **K_i = 0.89 ± 0.23** **(Competitive)**

1a	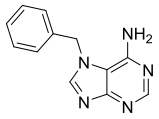	$PhCH_2$-(N7)	1.1	26 ± 10% (1 mM)
1b	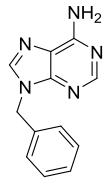	$PhCH_2$-(N9)	1.9	23 ± 4% (1 mM)
2a	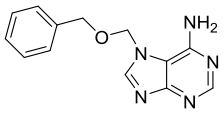	$BnOCH_2$- (N7)	1.1	No inhibition (1 mM)
2b	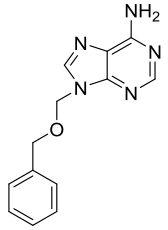	$BnOCH_2$- (N9)	1.9	13 ± 3% (1 mM)
6a	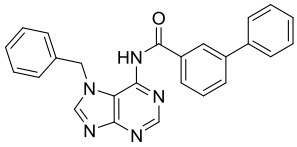	**$PhCH_2$-(N7)**	**4.3**	**52 ± 2%**
6b	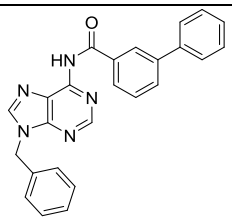	**$PhCH_2$-(N9)**	**5.1**	**57 ± 9%**
7a***	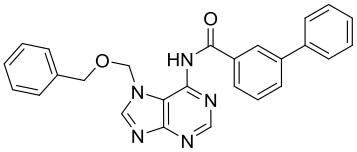	**$BnOCH_2$- (N7)**	**4.2**	**50 ± 1%**
7b	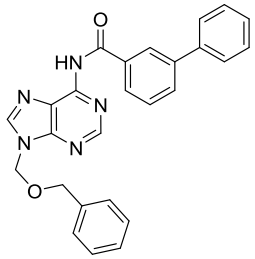	$BnOCH_2$- (N9)	5.0	34 ± 4%

3	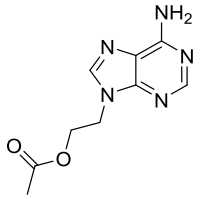	(N9)	0.4	No inhibition (1 mM)
4	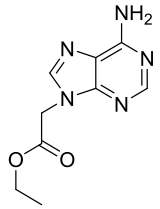	(N9)	0.5	3 ± 3%
5	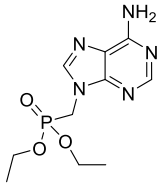	(N9)	0.3	No inhibition (1 mM)
8	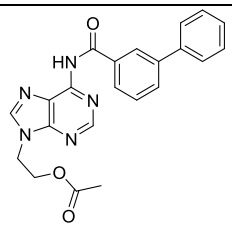	**(N9)**	**3.6**	**62 ± 4%**
11	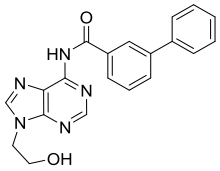	(N9)	2.8	46 ± 7%
9	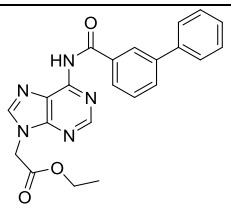	**(N9)**	**3.7**	**60 ± 1%**
12	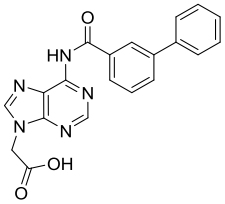	**(N9)**	**2.7**	**62 ± 4%** **K_i = 0.84 ± 0.16** **(competitive)**
10	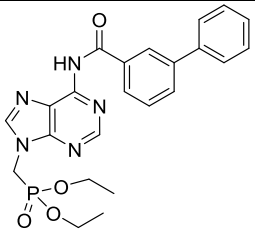	(N9)	3.5	47 ± 5%

13	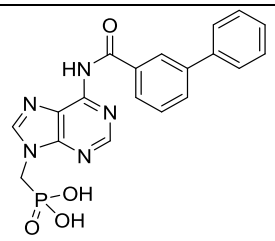	(N9)	2.2	n.a. K_i = 2.4 ± 0.41 (competitive)

*clogP values were calculated with MolInspiration (freely available online software: http://www.molinspiration.com/cgi-bin/properties)

**Data for UA2132 are from [19]. n.a. when precipitation occurs upon addition of the green malachite reagent. Compounds promoting significant enzyme inhibition are indicated in bold.

*** Compound 7a was 81.8% pure.

Table 2. Data for analogues incorporating a polar substituent on the imidazole ring

Compound	Structure	*N-7* / *N-9* substituent	**cLogP***	Inhibition (%) at 200 μM K_i (mM)
18	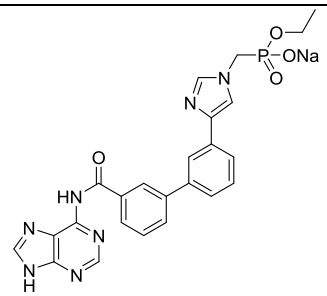	**None**	**2.5**	**75 ± 5%** **K_i= 0.58 ± 0.08** **(competitive)** **Single negative charge as Ilib-72**
20	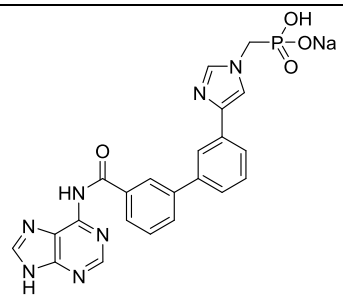	None	1.8	49 ± 4%
19	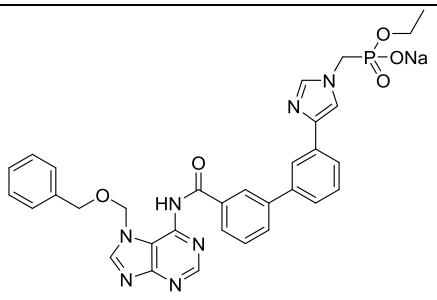	**BnOCH$_2$-(N7)**	**3.33**	**60 ± 5%**

Compounds promoting significant enzyme inhibition are indicated in bold

*clogP values were calculated with MolInspiration (freely available online software: http://www.molinspiration.com/cgi-bin/properties)

Finally, tetrazolo derivative **24c** (and to a lower extend **24b**) was a good mimicry of carboxylate group, when introduced in the *meta* or *para* orientation, confirming the improvement observed with a carboxylate group which promotes an increased solubility of these compounds associated with an enhanced activity (Table 3). According to the position of the tetrazolo group (*ortho*, *meta* or *para* regarding to the biaryl group), there was a large difference in terms of enzymatic inhibition. The most favorable substitution was in the *para* position (**24c**) followed by *meta* with less efficiency (**24b**).

Table 3. Data for analogues incorporating a tetrazole as five-membered ring

Compound	Structure	*N-7* / *N-9* substituent	**cLogP***	Inhibition (%) at 200 µM K_i (mM)
24a	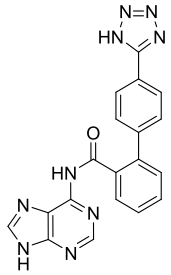	None	2.8	30 ± 4%
24b	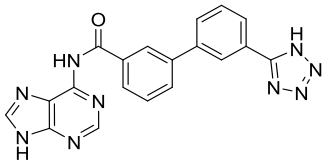	**None**	**2.8**	**50 ± 2%**
24c	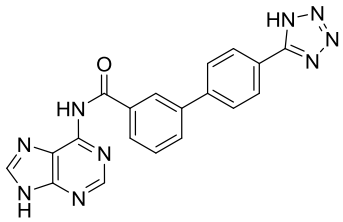	**None**	**2.8**	**60 ± 3%**
24d	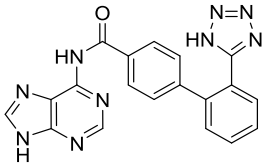	None	2.8	10 ± 2%
24e	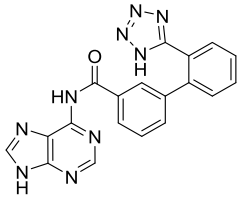	None	2.8	27 ± 5%

25	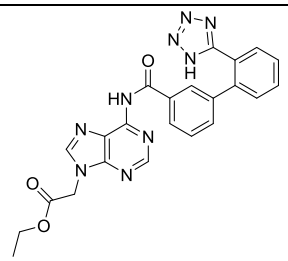	(N9)	3.1	27 ± 6%

Compounds promoting significant enzyme inhibition are indicated in bold
*clogP values were calculated with MolInspiration (freely available online software: http://www.molinspiration.com/cgi-bin/properties)

Thus, inhibition of the 5'-nucleotidase activity was observed for ten derivatives, showing 50 to 75% inhibition of the purified recombinant protein at 200 µM. Among these, two derivatives (**12** and **18**) were further studied to determine inhibition constants and mode of inhibition. They both exhibited K_i in the sub-millimolar range, respectively 0.84 and 0.58 mM (Fig. 6) and were found as competitive inhibitors (Figure S1). In addition, they appeared as potent as our reference compound **UA2132** (K_i =0.89 mM) with a slight advantage for **18** which is very close to the **Ilib-72** chemical structure.

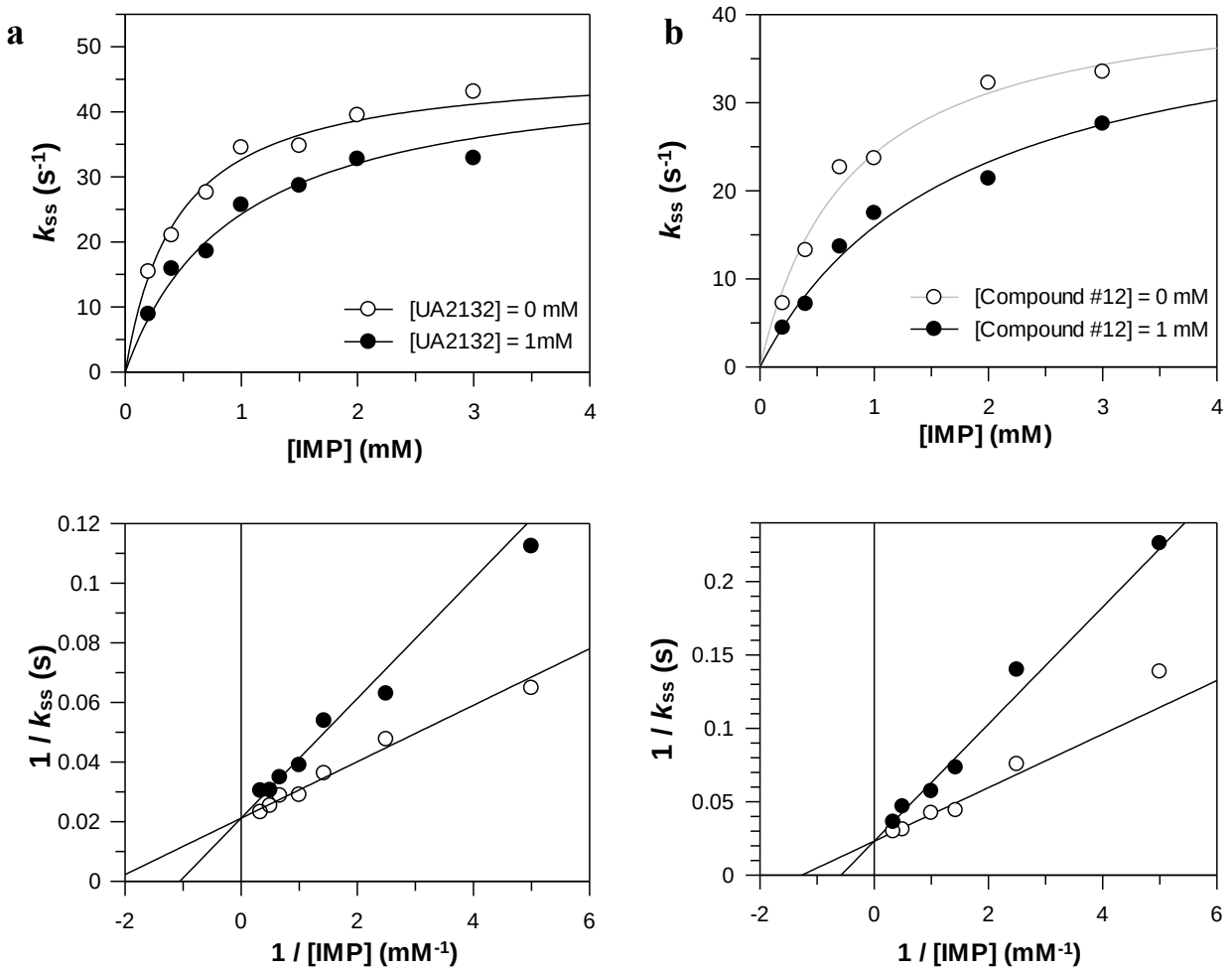

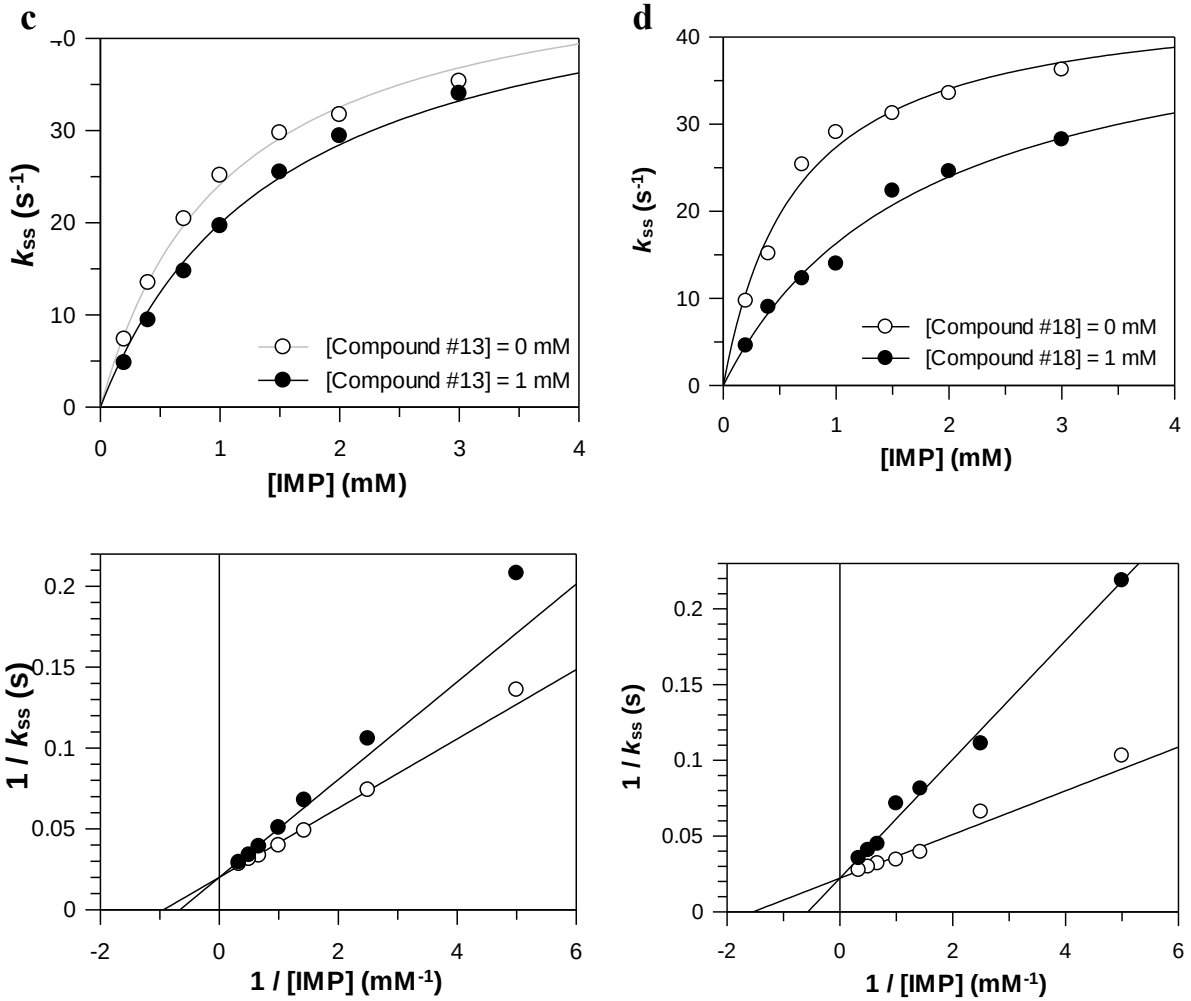

Figure 6. Michaelis-Menten kinetic profiles (with the corresponding Lineweaver-Burk plots) obtained by using a competitive inhibition mode for compounds **UA2132** (a), **12** (b), **13** (c) and **18** (d). Analysis of the kinetic inhibition curves (inhibition modes and equations used for fitting) are detailed in supporting information.

Crystallography. A selection of the potential inhibitors (depending on their *in vitro* activity, availability and solubility) was used for co-crystallization and soaking experiments at final ligand concentrations of 5 and 10 mM. Diffraction data were collected on crystals soaked in solutions containing **UA2132**, **2a**, **7a**, **12** and **20**, respectively. All crystal structures solved within this study, display the same overall fold as those previously reported with an α/β core-domain and a cap-domain (Figure 7). Of the various studied crystal structures (Table S3) only those determined from crystals soaked in a solution containing 10 mM of **2a** or **UA2132** displayed electron densities which partly could be interpreted as being the two respective ligand (Fig. S2), at least in regions being visible within the electron density map. Indeed, the region 401-416 is always reported as being highly

disordered in form I crystals [15, 22, 25] whereas it was visible in the electron density of form II crystals [19].

When taking the data from the previous enzyme kinetic studies into account, one cannot exclude binding of the other flexible parts of the enzyme for the other molecules for which electron density is lacking, at least for **2a**, **13** and **18** for which no crystals could be obtained by co-crystallization in either forms.

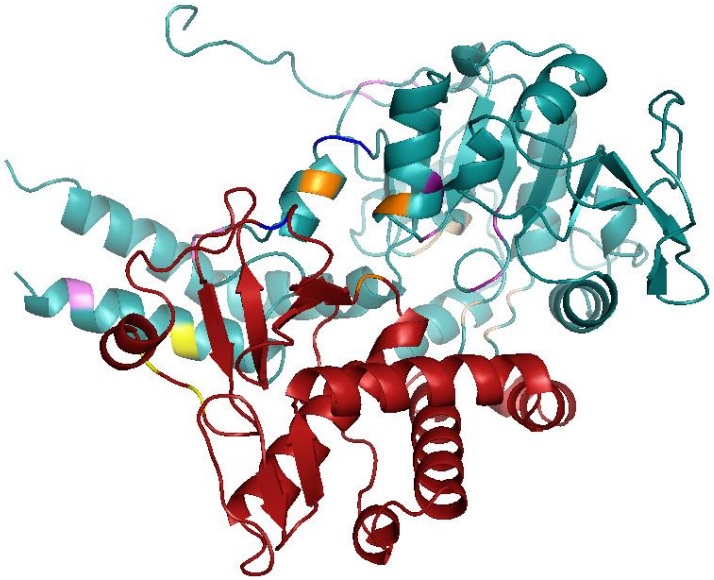

Figure 7. Overall three-dimensional structure of cN-II with the core-domain colored in red and the cap-domain colored in teal. Binding sites observed so far within various crystal structures are in purple the active site [22], in orange the "AdiS" binding site,[15] in dark blue effector site 1 and in yellow effector site 2 [25], in wheat the "2c" site and in pink spanning over a longer range the "3c" binding site [19].

Binding mode prediction to understand the inhibition mechanism. As no crystal structure with a ligand bound in an unequivocal manner could be obtained, molecular docking was used to understand the mechanism by which the most efficient compounds inhibit the enzyme. Compounds **12** and **13** exhibit very similar binding modes as predicted by docking (Fig. 8A). Both compounds were found superimposed in the active site with the carboxylic or phosphoric acid chain pointing towards the magnesium ion. This prediction cannot explain the difference in terms of enzymatic inhibition (K_i of 0.84 and 2.4 mM, respectively). However, the docking score was a good indication of the binding strength with 112.6 versus 145.9 for the carboxylic acid group and the phosphoric acid chain, respectively. This stronger theoretical binding affinity for derivative **13** can be easily explained by the overall negative charge of the compound (-2) and it should have been predicted as a

better inhibitor. However, and according to the inhibition values, the inhibition efficiency seems to be governed by a more complicated mechanism. One can imagine that the higher water solubility of compound **13** may prevent or limit the access to the target binding site as the surrounding residues are aromatic (F157, H209 and Y210) and also because best inhibitors were highly hydrophobic. When comparing their binding mode with Ilib72 (Fig. 8B), no obvious similarity was observed with a large shift of the biaryl moiety likely due to the differential positioning of the negative charge on these compounds.

In contrast to compounds **12** and **13**, the overlay between Ilib-72 and **18** or **20** (Fig. 8C) showed interesting resemblances with nearby positioning of their adenine and biaryl groups. Intriguingly, derivative **18** was determined more active *in vitro* than **20**. This raises the question about the overall negative charge of the compound and may indicate that a single negative charge is more suitable for enzymatic inhibition (identically to Ilib-72). Interestingly, the coordination of the magnesium ion changed depending on the compound (**18** or **20**), probably due to the different electron distribution around the phosphate-bound oxygen atoms. Several water molecules were displaced and involved in this coordination. Moreover, an important hydrogen bond network formed between the carbonyl oxygen and water molecule is present for compound **18** while these interactions are absent for compound **20** (Fig. 8D).

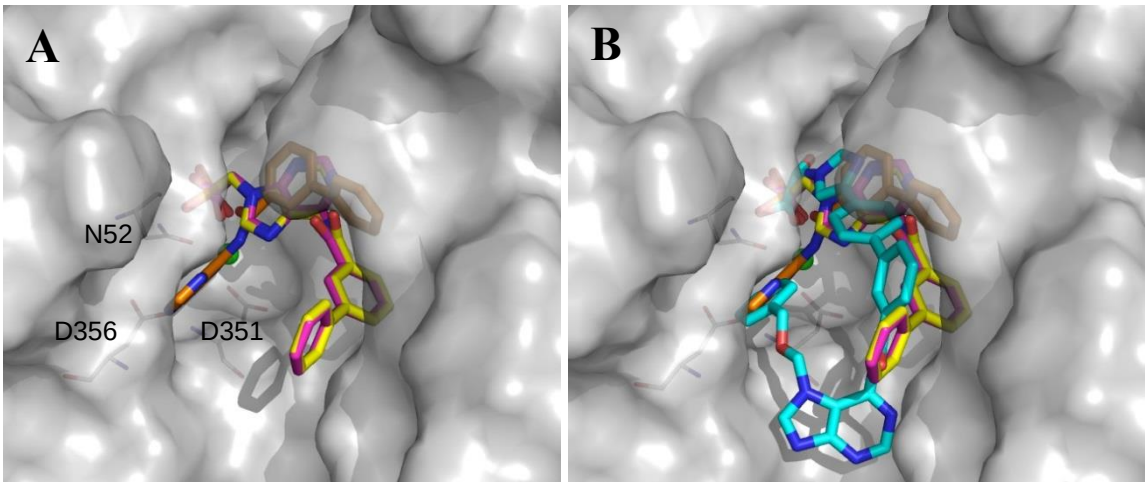

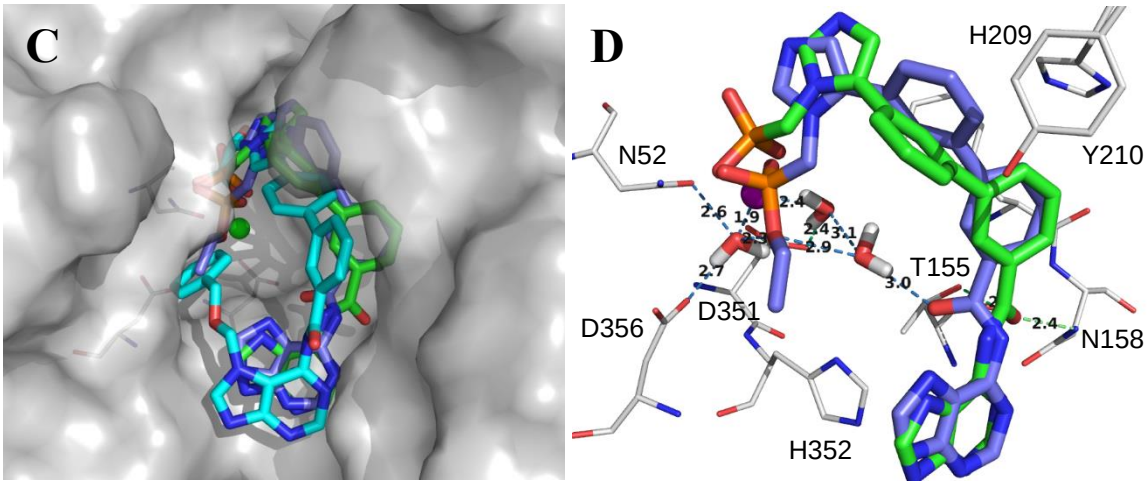

Figure 8. Prediction of the binding modes of selected compounds by docking on 2XCW structure. (A) Superimposition of **UA2132** (orange), **12** (pink) and **13** (yellow) with negative charge near Mg^{2+} ion. (B) Same as in A with Ilib-72 (cyan sticks). (C) Binding modes of compounds **18** (blue), **20** (green) and Ilib-72 (cyan sticks). (D) Hydrogen bonding network with water molecules connecting compound **18** (blue stick) to the magnesium ion (depicted as a purple sphere) whereas compound **20** is making only hydrogen bonds with N158 and T155.

Concerning derivatives **24a-e** incorporating a tetrazole group, their binding orientation seems to be governed by this group. Indeed, its interaction with the magnesium ion is thought to be strong and the orientation of the rest of the molecule will depend on the *ortho*, *meta* or *para* position of this substituent on the biaryl skeleton (Fig. 9A). Indeed, the five derivatives were predicted with the tetrazolo group near the metallic ion with various orientation of the adenine moiety depending on biaryl substitution. According to the docking predictions, compounds **24a**, **24d** and **24e** bind to the enzyme in a complete different manner, which may indicate a large variation in their binding affinity. Attempting to explain the higher efficacy of compound **24c** compared to **24b** (Fig. 9B), a similar hypothesis as previously expressed for compounds **18** and **20** can be postulated with the implication of water molecules reinforcing the interactions between protein amino acids and the inhibitor (Fig. 9B).

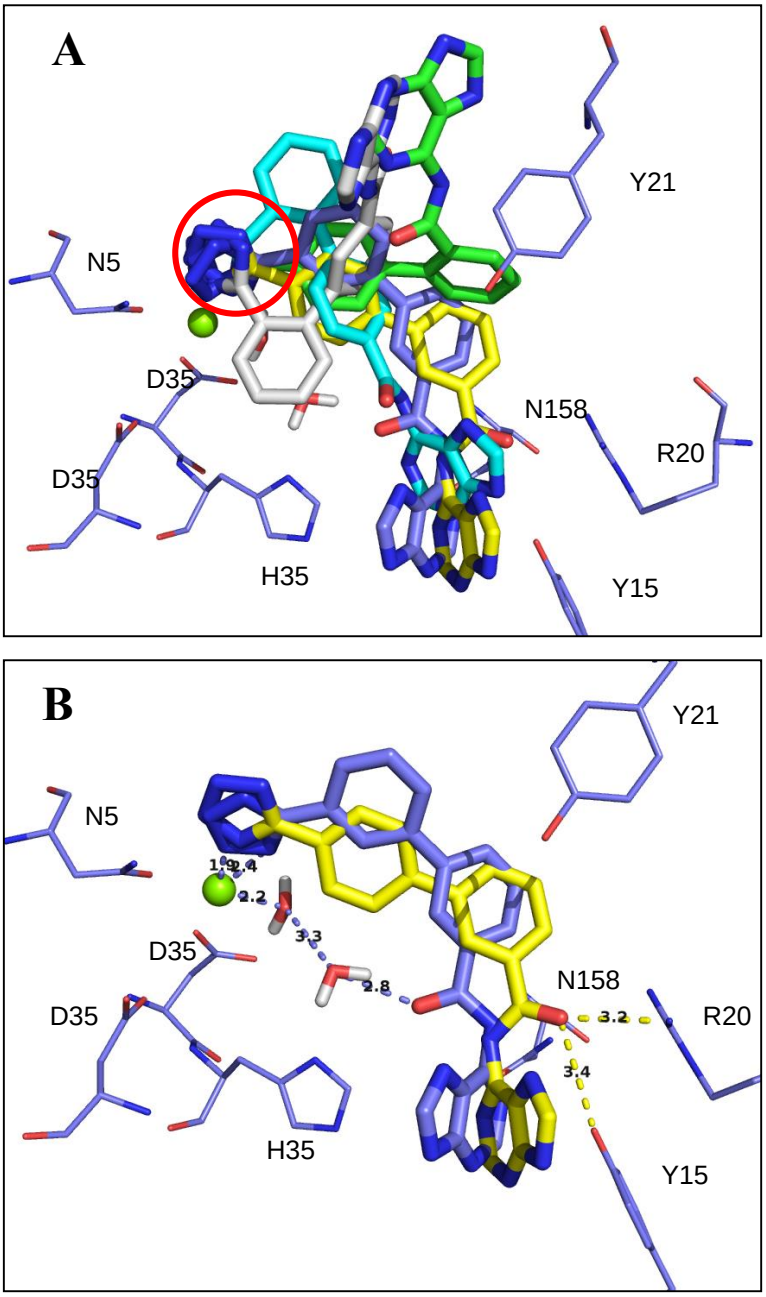

Figure 9. (A) Effect of the tetrazole group (highlighted by a red circle) on the final orientation of derivatives **24a** (green), **24b** (blue), **24c** (yellow) and **24d** (cyan) and **24e** (white). (B) Close-up view of the binding mode prediction of the two most active compounds from the tetrazolo series, **24b** (blue) and **24c** (yellow). The magnesium ion is depicted as a green sphere and surrounding protein amino acids are in thin sticks. Distances are color-coded for each compound.

***In vitro* biological evaluation.** The effect of the newly synthesized compounds was evaluated on the survival of different human cancer cell lines using a MTT (3-(4,5-dimethylthiazol-2-yl)-2,5-diphenyltetrazolium bromide) based colorimetric assay (Table S4). IC_{50} values ranged from 36 µM to >300 µM, similarly as for compounds previously reported [19]. Four *N*7- or *N*9-substituted

compounds (**6a**, **6b**, **7a** and **10**) and one tetrazolo-compound (**24c**) had IC_{50} below 100 μM on RL cells. These derivatives showed cN-II inhibition of approximately 50% at 200 μM and cLogP values allowing diffusion through cell membrane (>2.8), but there was no clear structural explanation of this antiproliferative activity in regard to cN-II inhibition.

Intrinsic antiproliferative activity allowed us to perform synergy experiments with selected compounds and purine nucleoside analogues as our hypothesis states that cN-II inhibitors would enhance the effect of cytotoxic nucleoside analogues in co-exposure conditions (Fig. 10). Synergy (defined as CI95<0.9) was observed with cladribine for **6a** (RL and HL-60), **6b** (CCRF-CEM and HL-60), **7a** (RL) and **10** (RL), with clofarabine for **6a** (RL), **6b** (HL-60) and **7a** (RL) and with fludarabine for **6a** (RL and CCRF-CEM) and **6b** (RL, CCRF-CEM and HL-60). The differences between the cell lines is consistent with earlier observations showing that shRNA-mediated cN-II inhibition is associated with a higher level of sensitization to purine nucleoside analogues in RL and HL-60 cells as compared to CCRF-CEM cells [10]. Thus, based on these results, **6a** could be considered as a good candidate and clearly better than our previous inhibitor (**UA2132**). It is however noteworthy that no co-incubation experiments with non-toxic compounds were performed and could have allowed the identification of other active associations.

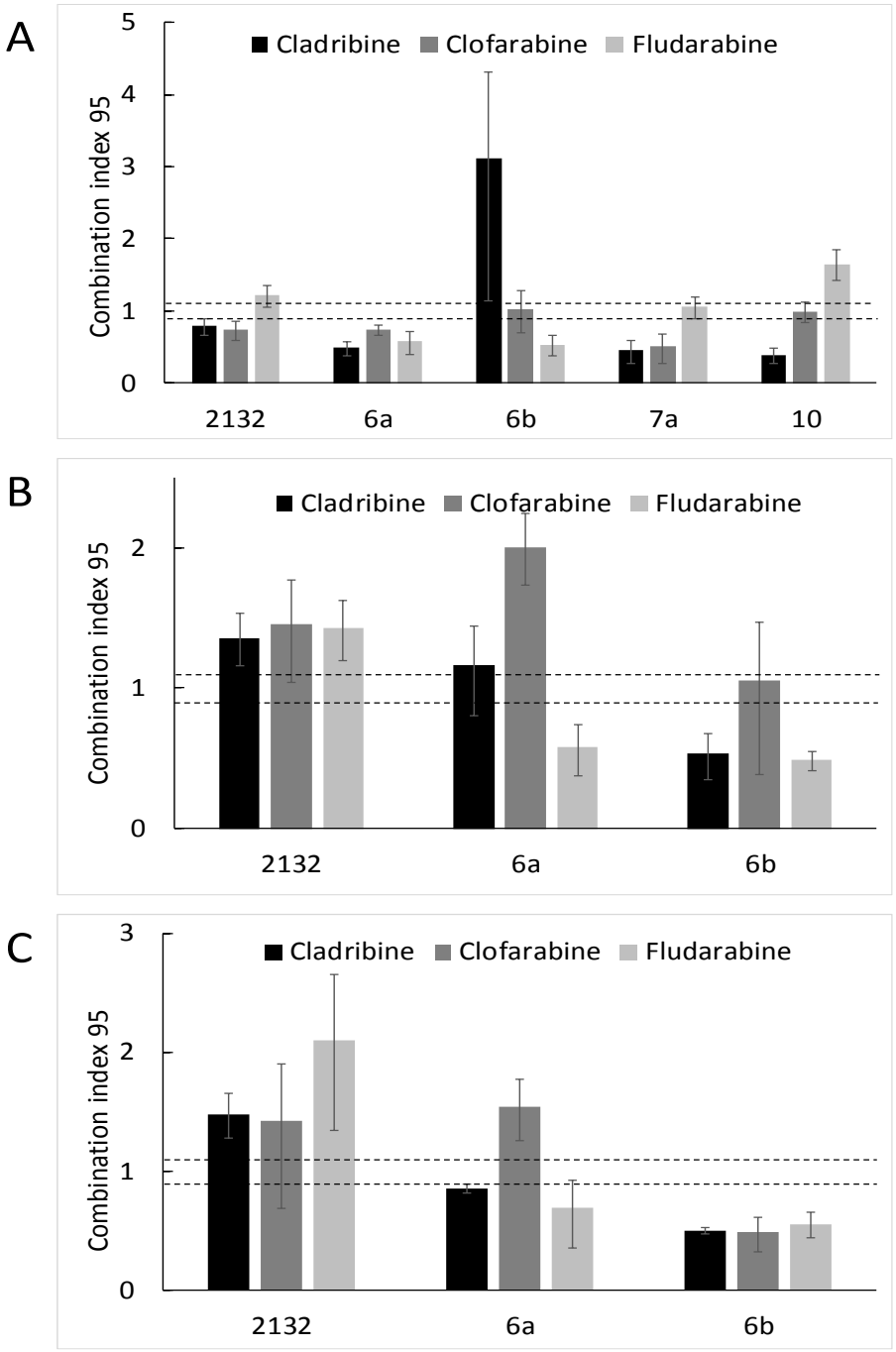

Figure 10. Combination index 95 for associations of purine nucleoside analogues cladribine (black bars), clofarabine (dark grey bars) or fludarabine (light grey bars) and cN-II inhibitors on RL (A), CCRF-CEM (B) and HL-60 (C) cells. CI_{95} values (a parameter for the quantification of the combinatory effect of the two compounds to achieve 95% inhibition of cell survival) were calculated with the CompuSyn software based on the Chou and Talalay method [29] as indicated in Material and Methods, and expressed as 10^(mean(logCI_{95})) from at least three independent experiments.

Error bars indicate CI_{95}-SEM and CI_{95}+SEM. Drug combinations with $CI_{95} < 0.9$ are considered synergistic, whereas they are additive for $0.9 < CI_{95} < 1.1$ and antagonistic for $CI_{95} > 1.1$.

CONCLUSION

By using a combination of various *in silico* approaches, we designed a large chemical library of potential cN-II inhibitors with numerous different scaffolds of which some leading to inaccessible chemical synthesis. Consequently, we focused on the structural optimization of a previously characterized inhibitor that was also part of the Ilib-generated compound (**Ilib-72**). This allowed us to explore the chemical diversity of this lead compound in order to improve its affinity for the targeted protein and/or physico-chemical properties such as solubility. Twenty-six derivatives were synthesized, evaluated toward the purified recombinant enzyme. About ten compounds could inhibit more than 50% of the enzymatic activity at a concentration of 200 µM. In comparison with our reference compound (**UA2132**, a previously identified competitive inhibitor), three derivatives (**12**, **13** and **18**) displayed similar potency, with K_i in the micromolar range and a competitive mechanism of action. All three compounds have a polar and anionic substituent (either a carboxylate or a phosphonate) and derivative **18** presented the closest structural similarity with **Ilib-72**, the derivative selected from the library generation and *in silico* screening process. Molecular modelling and X-ray crystallography studies were carried out to predict and assess the binding modes of these novel derivatives. When tested in cell culture experiments, synergistic effects were observed with all cytotoxic nucleoside analogues tested and compounds **6a-b**. Some compounds had minor cytotoxicity, and their complete toxicity profile on non-cancerous cells will be needed for further development. These results are therefore encouraging to investigate further the potential of these compounds as to our knowledge they appeared as the most potent cN-II inhibitors reported to date.

EXPERIMENTAL SECTION

Library generation and molecular docking studies. Using hit fragments previously identified by NMR screening [19], a focused library of final compounds targeting cN-II was generated using Ilib-diverse program (www.inteligand.com) by randomly assembling three different hit fragments. A weighting percentage has been attributed for the fragments that were previously identified as cN-II inhibitors (Table S1 in SI). In addition, several functional or polar groups were included to increase the solubility of the final compounds (hydroxyl, sulfonate, phosphate and phosphonate groups). This procedure allowed us to generate 3,000 compounds supposed to be chemically synthesizable (the program includes general rules of chemical synthesis during the linkage process). All derivatives

were analyzed and their coordination and geometry corrected by using the VegaZZ molecular modelling program [30]. Atomic charges were assigned using the Gasteiger-Marsili empirical atomic partial charges [31] and the potential energy of all compounds was minimized using 500 steps of steepest descent followed by 5,000 steps of conjugate gradient (tolerance of 0.01 kcal/mol. Å). For compounds comprising a tetrazole group, only one tautomer has been evaluated by docking. Molecular docking was carried out with the GOLD v5.2 program (Genetic Optimization for Ligand Docking) from Cambridge Crystallographic Data Centre (CCDC) Software Limited [32, 33] with partial flexibility of protein amino acid sidechains and full flexibility of Ilib-diverse generated compounds. Docking was performed on the cN-II crystal structure in which the nucleotidase was complexed with IMP (PDB 2XCW) by applying 50 genetic algorithm steps for conformational poses searching with a radius of 12 Å around the target atom, Mg^{2+} ion (located in the substrate binding site). Although the 2XCW crystal structure harbors the D52N mutation, it was chosen among the numerous available structures because of the accurate characterization of the substrate binding mode. Our earlier docking studies performed using the 2JC9 structure without substrate bound in the active site and compared to those performed using 2XCW in this study showed highly similar results, thus giving a proof-of-concept for using this structure of an inactive mutant. Structural water molecules present in the crystal structure near the IMP binding site were retained and allowed to contribute with a 2 Å cut-off of translational and rotational freedom. Docking poses were analyzed by the clustering method (complete linkage) from the rmsd matrix of ranking solutions. Solutions were classified according to their respective scores calculated by the Goldscore scoring function. Structural analysis and visualization of docking poses were achieved with the PyMOL Molecular Graphics System (version 1.3, Schrödinger, LLC).

Enzyme inhibition and steady state kinetics assays. The nucleotidase activity was measured using the Green Malachite Phosphate Assay kit (Gentaur) as previously described [16, 19]. Briefly, in 96-wells plate arranged on ice, recombinant purified cN-II was added to a final concentration of 0.1 µM in 80 µL buffer containing 50 mM imidazole pH 6.5, 500 mM NaCl, 10 mM $MgCl_2$ and then incubated for 10 min with the different compounds to be evaluated as potential cN-II inhibitors. The reaction was started by addition of the substrate (50 µM of IMP with an equimolar amount of Mg) and incubated at 37° C for 5 min. The reaction was stopped by addition of 20 µL of Green malachite reagent (strong acid) and free phosphate was quantified by reading the absorbance at 630 nm on a plate reader (Tecan Sunrise). The percentage of enzymatic inhibition has been calculated by using the following formula: % inhibition = 1 - [(x – Min) / (Max - Min)]. Min and Max refer to the absorbance of full-inhibition and Max the signal in absence of inhibitor, respectively. For the most

active compounds, Michaëlis-Menten kinetics were performed to determine the inhibition mode and inhibition constants, as previously described [19]. Briefly, enzyme (alone or in presence of compounds) and substrate (IMP at different concentrations varying from 0.2 to 3 mM) were mixed in a thermostatically controlled beaker under magnetic stirring at 37 °C (same buffer as for the previous assay). Every 7 s, samples were taken from the mixture and reaction was stopped by adding 10% of perchloric acid. Quantification of IMP and inosine was performed by HPLC (Waters Alliance) using a Partisphere 5-SAX column (AIT France) and 10 mM ammonium phosphate buffer pH 5.5 as mobile phase. The raw data (IMP and inosine peaks area integrated with Empower software, Waters) were analyzed using Grafit 7 (Erithacus Software) and fitted with equations describing either a competitive, a non-competitive, an uncompetitive or a mixed inhibition mechanism. The equation that reproduced best the experimental data was selected for the determination of the inhibition mode by also taking into account the chi square value (confidence computed from the fitting giving the independence statistical test between experimental and theoretical values).

Cell-based experiments. Cell survival in presence of cN-II inhibitors and purine nucleoside analogues alone (intrinsic cytotoxicity) or in combination (synergy experiments) was determined with human follicular lymphoma cells (RL), human acute lymphoblastic leukemia cells (CCRF-CEM) and human acute promyelocytic leukemia cells (HL-60). as described earlier [15, 19]. Briefly, ten thousand cells were seeded per well in 96-well plates and incubated with different concentrations of drugs and inhibitors alone or in fixed ratio combinations for 72 hours, and cell survival was determined with the MTT assay. Inhibitory concentrations 50 (IC_{50}, concentrations associated with 50% cell survival as compared to unexposed cells) and combination index 95 (CI_{95}, a parameter for the quantification of the combinatory effect of the two compounds to achieve 95% inhibition of cell survival) were calculated with the CompuSyn software based on the Chou and Talalay method. [29] Drug combinations with $CI_{95} < 0.9$ are considered synergistic, whereas they are additive for $0.9 < CI_{95} < 1.1$ and antagonistic for $CI_{95} > 1.1$.

Crystallization, data reduction, structure determination and refinement. Protein used for X-ray crystallography studies was prepared as described earlier [34] and concentrated to 8 mg/ml for crystallization. All compounds used for crystallization were dissolved in 1% DMSO to a concentration of 50 mM. Both nanoliter- (1:1 ratio of 200 nL protein: reservoir solution employing a Mosquito™ robot (TTP Labtech) with 96 well plates and microliter crystallization experiments with 24 well plates were performed using the sitting drop vapor diffusion method, and “form I” [22]) and “form II” [19] experimental conditions. Freshly purified C-terminal truncated cN-II (see ref. [15] 8

mg/mL) was mixed with compounds **UA2132**, **2a**, **7a**, **12**, **13**, **18** and **20** to final concentrations of 5 and 10 mM of these latter and incubated at 4 °C for 20 minutes prior to co-crystallization setup. Crystals grown in the presence of compounds (co-crystallization) appeared upon 1-2 weeks. Only compounds **7a** and **20** could be co-crystallized, and in forms II and I, respectively. For soaking experiments (conducted in parallel), native crystals (both forms) appeared after approximately one week at 4 °C. Only form I crystals were further studies due to an extreme fragility of form II crystals which fell apart upon soaking. For cryo-protection, crystals were transferred to a drop containing the crystallization reservoir solution (at the above mentioned conditions) supplemented with 10% and 15% glycerol for "form I" and "form II" crystals, respectively, and flash-frozen in liquid nitrogen. Hereafter, X-ray diffraction data were collected at the European Synchrotron radiation facility (ESRF Grenoble France), and integrated and scaled using programs from the XDS package [35]. All crystal structures were determined using the molecular replacement method and the program "Phaser" [36] as implemented in the "Phenix" software suite [37] and the previously reported cN-II structures (2J2C) [22] and (5CQZ) [19] as search models for forms I and II, respectively. Refinement was performed using the programs "Refmac5" [38] and "Phenix" [37], altering with iterative model re-building and analysis with "COOT" [39]. Ligands and water molecules displayed 2Fo-Fc and Fo-Fc electron densities contoured at the 1σ and 3σ level, respectively, prior to refinement. The pdb coordinates and topology of the compounds tested for binding during refinement (though lacking in final three-dimensional structures) were obtained using the PRODRG2 server [40] and the program "eLBOW" as implemented in "Phenix". Libraries for refinement of these molecules were generated using the program LIBCHECK as implemented in the CCP4 program package [41]. Composite omit maps were calculated ("Phenix") in order to reduce model bias, and rmsd's were calculated with the program TM-score [42]. Data collection and refinement statistics are given in Table S3.

Coordinates and structure factors of the cN-II structures have been deposited at the RCSB (Research Collaboratory for Structural Bioinformatics) Protein Data Bank (http://www.rcsb.org) under the entry codes 6FIR (cN-II-2132, 5 mM), 6FXH (cN-II-2132, 10 mM), 6FIS (cN-II-**2a**), 6FIW (cN-II-**20**) and 6FIU (cN-II-**12**), respectively.

Description of general methods for chemical synthesis is already published [19]

Diethyl *p*-toluenesulfonyloxymethylphosphonate [28], compounds **1a-b**, [43], **2a-b** [44], **3** [45] and **4** [46] were prepared according to previously published procedures.

General Procedure for Synthesis of Compounds (1-4). To a stirred solution of adenine (7.40 mmol) in DMF (30 mL) was added under argon dry K_2CO_3 (10.73 mmol) and the corresponding alkyl halide (8.88 mmol). The mixture was stirred at room temperature until thin layer chromatography (TLC) revealed that the starting material was consumed. The solvent was evaporated under reduced pressure and the residue was purified on silica gel column chromatography (CH_2Cl_2/MeOH, 0-10%) to provide compounds **1-3** whereas compound **4** was isolated after precipitation in water and filtration.

7-Benzyl-7H-adenine (**1a**): yield = 20 %; white powder; ^{1}H NMR (DMSO-d_6): δ = 5.50 (s, 2H), 7.29-7.36 (m, 3H), 7.44-7.46 (m, 2H), 7.75 (s, 1H), 7.95 (bs, 2H), 8.55 (s, 1H); MS (ESI) *m/z* 226.0 $[M+H]^+$.

9-Benzyl-9H-adenine (**1b**): yield = 24 %; white powder; ^{1}H NMR (DMSO-d_6): δ = 5.36 (s, 2H), 7.24-7.33 (m, 7H), 8.14 (s, 1H), 8.25 (s, 1H); MS (ESI) *m/z* 226.1 $[M+H]^+$.

7-Benzyloxymethyl-7H-adenine (**2a**): yield = 43 %; white powder; ^{1}H NMR (DMSO-d_6): δ = 4.70 (s, 2H), 5.79 (s, 2H), 7.30 (s, 5H), 7.79 (s, 1H), 8.12 (bs, 2H), 8.48 (s, 1H); MS (ESI) *m/z* 256.1 $[M+H]^+$.

9-Benzyloxymethyl-9H-adenine (**2b**): yield = 22 %; white powder; ^{1}H NMR (DMSO-d_6): δ = 4.58 (s, 2H), 5.63 (s, 2H), 7.29-7.32 (m, 7H), 8.20 (s, 1H), 8.31 (s, 1H); MS (ESI) *m/z* 256.0 $[M+H]^+$.

2-(Adenin-9-yl)ethyl acetate (**3**): yield = 60 %; white powder; ^{1}H NMR (DMSO-d_6): δ = 1.97 (s, 3H), 4.42 (s, 4H), 7.27 (bs, 2H), 8.17 (s, 2H); MS (ESI) *m/z* 222.0 $[M+H]^+$.

Ethyl-2-(adenin-9-yl) acetate (**4**): yield = 28 %; white powder; ^{1}H NMR (DMSO-d_6): δ = 1.12 (t, 3H, ^3J = 7.2 Hz), 4.07 (q, 2H, ^3J = 7.2 Hz), 4.97 (s, 2H), 7.18 (bs, 2H), 8.02 (s, 1H), 8.04 (s, 1H); MS (ESI) *m/z* 222.2 $[M+H]^+$.

Synthesis of 9-(diethoxyphosphorylmethyl) adenine (**5**): To a stirred solution of adenine (7.40 mmol) in DMF (45 mL) was added under argon NaH 60% (8.90 mmol) and diethyl p-toluenesulfonyloxymethylphosphonate (8.97 mmol). The mixture was stirred at 50 °C for 17 h. The solvent was evaporated and the residue was purified on silica gel column chromatography (CH_2Cl_2/MeOH, 0-10%) to provide compound **5** in a 56% yield as a white powder; ^{1}H NMR (DMSO-d_6): δ = 1.19 (t, 6H, ^3J = 7.2 Hz), 4.08 (q, 4H, ^3J = 7.2 Hz), 4.74 (d, 2H, ^3J = 11.6 Hz), 7.36 (bs, 2H), 8.08 (s, 1H), 8.21 (s, 1H); ^{31}P NMR (DMSO-d_6): δ = 19.0; MS (ESI) *m/z* 286.1 $[M+H]^+$.

General Procedure for Synthesis of Compounds (6-10). To a stirred solution of *N*7- or *N*9-substituted adenine derivatives **1a**, **1b**, **2a**, **2b**, **3**, **4** or **5** (1.05 mmol) in pyridine (3 mL) was added portion wise under argon the biphenyl-3-carbonyl chloride (1.15 mmol). The solution was stirred at

rt or 100 °C until TLC revealed that the starting material was consumed. Solvents were removed under reduced pressure and the residue was purified on silica gel column chromatography (CH_2Cl_2/MeOH, 0-10%) to provide compounds **6-10**. Additional precipitation of a methanolic solution of compounds **7a** and **7b** in diethyl ether was required to obtain samples with sufficient purity.

***N*-(7-Benzyl-7*H*-purin-6-yl)-[1,1'-biphenyl]-3-carboxamide** (**6a**): yield = 94 %; white powder; ^{1}H NMR (DMSO-d_6): δ = 5.95 (s, 2H), 7.41-8.19 (m, 13H), 8.48 (s, 1H), 8.99 (s, 1H), 9.71 (s, 1H), 13.33 (bs, 1H); ^{13}C NMR (DMSO-d_6): δ = 51.3, 113.5, 124.5 (2C), 125.0, 125.6, 125.7, 126.0 (2C), 126.2, 126.3 (2C), 126.6 (2C), 127.0, 129.4, 129.9, 131.7, 136.6, 137.9, 144.5, 146.5, 146.7, 149.9, 164.3; MS (ESI) *m/z* 406.2 $[M+H]^+$; HRMS: calcd for $C_{25}H_{20}N_5O$ $[M+H]^+$ 406.1668, found 406.1675; HPLC t_R = 8.1 min, 98.5%.

***N*-(9-Benzyl-9*H*-purin-6-yl)-[1,1'-biphenyl]-3-carboxamide** (**6b**): yield = 59 %; white powder; ^{1}H NMR (DMSO-d_6): δ = 5.55 (s, 2H), 7.36-8.07 (m, 13H), 8.40 (s, 1H), 8.68 (s, 1H), 8.80 (s, 1H), 11.43 (bs, 1H); ^{13}C NMR (DMSO-d_6): δ = 44.4, 123.2, 124.5, 124.8 (2C), 125.4, 125.5 (2C), 125.7, 125.8, 126.7 (2C), 126.9 (2C), 127.1, 128.5, 131.9, 134.5, 137.3, 138.2, 142.6, 148.1, 149.5, 150.2, 163.3; MS (ESI) *m/z* 406.2 $[M+H]^+$; HRMS: calcd for $C_{25}H_{20}N_5O$ $[M+H]^+$ 406.1668, found 406.1653; HPLC t_R = 8.6 min, 97.3%.

***N*-(7-((Benzyloxy)methyl)-7*H*-purin-6-yl)-[1,1'-biphenyl]-3-carboxamide** (**7a**): yield = 12 %; white powder; δ = 4.72 (s, 2H), 5.88 (s, 2H), 7.30-7.76 (m, 11H), 7.89-8.03 (m, 2H), 8.29 (m, 2H), 8.71 (s, 1H), 12.56 (bs, 1H); ^{13}C NMR (DMSO-d_6): δ = 71.4, 78.2, 126.8 (2C), 127.1, 127.6 (2C), 127.8 (2C), 128.0 (2C), 128.3 (2C), 129.1 (2C), 130.4 (2C), 135.6, 137.1, 139.6, 140.2, 144.5, 149.9 (3C), 171.1; MS (ESI) *m/z* 436.3 $[M+H]^+$; HRMS: calcd for $C_{26}H_{22}N_5O_2$ $[M+H]^+$ 436.1774, found 436.1761; HPLC t_R = 6.9 min, 81.8% (unstable).

***N*-(9-((Benzyloxy)methyl)-9*H*-purin-6-yl)-[1,1'-biphenyl]-3-carboxamide** (**7b**): yield = 27 %; white powder; ^{1}H NMR (DMSO-d_6): δ = 4.64 (s, 2H), 5.79 (s, 2H), 7.31-7.56 (m, 8H), 7.66 (t, 1H, ^3J = 8.0 Hz), 7.82 (d, 2H, ^3J = 8.0 Hz), 7.94-8.05 (m, 2H), 8.38 (s, 1H), 8.68 (s, 1H), 8.82 (s, 1H), 11.40 (bs, 1H); ^{13}C NMR (DMSO-d_6): δ = 70.7, 72.2, 125.2, 126.7, 126.9 (2C), 127.5 (2C), 127.6, 127.7, 127.9 (2C), 128.3 (2C), 129.0, 129.2, 130.6, 133.9, 137.1, 139.3, 140.3, 144.9, 150.3, 152.0, 152.7, 163.3; MS (ESI) *m/z* 436.1 $[M+H]^+$; HRMS: calcd for $C_{26}H_{22}N_5O_2$ $[M+H]^+$ 436.1774, found 436.1762; HPLC t_R = 9.1 min, 97.7%.

2-(6-([1,1'-Biphenyl]-3-carboxamido)-9*H*-purin-9-yl)ethyl acetate (**8**): yield = 62 %; white powder; ^{1}H NMR (DMSO-d_6): δ = 1.98 (s, 3H), 4.49-4.59 (m, 4H), 7.44-8.18 (m, 8H), 8.41 (s, 1H), 8.55 (s, 1H), 8.80 (s, 1H), 11.41 (bs, 1H); ^{13}C NMR (DMSO-d_6): δ = 20.5, 42.5, 61.9, 125.2, 126.6, 126.9 (2C), 127.5, 127.9, 129.0 (2C), 129.2, 130.5, 134.0, 139.3, 140.3, 144.8, 150.1, 151.4, 152.6,

165.4, 170.1; MS (ESI) *m/z* 402.1 $[M+H]^+$; HRMS: calcd for $C_{22}H_{20}N_5O_3$ $[M+H]^+$ 402.1566, found 402.1565; HPLC t_R = 7.6 min, 98.8%.

Ethyl 2-(6-([1,1'-biphenyl]-3-carboxamido)-9*H*-purin-9-yl)acetate (**9**): yield = 57 %; white powder; ^{1}H NMR (DMSO-d_6): δ = 1.26 (t, 3H, ^3J = 7.0 Hz), 4.23 (q, 2H, ^3J = 7.0 Hz), 5.27 (s, 2H), 7.40-8.08 (m, 8H), 8.41 (s, 1H), 8.51 (s, 1H), 8.79 (s, 1H), 11.36 (bs, 1H); ^{13}C NMR (DMSO-d_6): δ = 14.0, 44.3, 61.5, 125.0, 126.7, 126.9 (2C), 127.6, 127.9, 129.0 (2C), 129.2, 130.6, 134.0, 139.4, 140.3, 145.1, 150.2, 151.7, 152.6, 165.5, 167.7; MS (ESI) *m/z* 402.2 $[M+H]^+$; HRMS: calcd for $C_{22}H_{20}N_5O_3$ $[M+H]^+$ 402.1566, found 402.1561; HPLC t_R = 8.0 min, 100%.

Diethyl ((6-([1,1'-biphenyl]-3-carboxamido)-9*H*-purin-9-yl)methyl)phosphonate (**10**): yield = 42 %; white powder; ^{1}H NMR (DMSO-d_6): δ = 1.21 (t, 6H, ^3J = 6.8 Hz), 4.08-4.16 (m, 4H), 4.91 (d, 2H, ^3J = 11.6 Hz), 7.30-8.10 (m, 8H), 8.42 (s, 1H), 8.43 (s, 1H), 8.83 (s, 1H), 11.41 (bs, 1H); ^{13}C NMR (DMSO-d_6): δ = 16.1 (2C,), 37.0 , 62.5 (2C), 124.7, 126.7, 126.9 (2C), 127.5, 127.9, 129.0 (2C), 129.2, 130.6, 134.0, 139.3, 140.3, 144.4, 150.3 151.6, 152.2, 165.4; ^{31}P NMR (DMSO-d_6): δ = 18.6; MS (ESI) *m/z* 466.3 $[M+H]^+$; HRMS: calcd for $C_{23}H_{25}N_5O_4P$ $[M+H]^+$ 466.1644, found 466.1631; HPLC t_R = 8.0 min, 99.5%.

General Procedure for Synthesis of Compounds (11) and (12). To a stirred solution of compound **8** or **9** (0.40 mmol) in MeOH (2 mL) at 0 °C was added a solution of NaOH 2M (4.0 mmol). The solution was stirred at 0 °C for 30 min and then the mixture was acidified until pH 1 with a solution of HCl 4M. The precipitate was filtered, washed with water, and dried to provide compound **11** or **12**.

***N*-(9-(2-Hydroxyethyl)-9*H*-purin-6-yl)-[1,1'-biphenyl]-3-carboxamide** (**11**): yield = 66 %; white powder; ^{1}H NMR (DMSO-d_6): δ = 3.87 (m, 2H), 4.45 (m, 2H), 7.45-7.60 (m, 3H), 7.71 (t, 1H, ^3J = 7.8 Hz), 7.84-8.11 (m, 4H), 8.45 (s, 1H), 8.92 (s, 1H), 9.04 (s, 1H); ^{13}C NMR (DMSO-d_6): δ = 47.0, 58.5, 119.4, 126.9 (3C), 127.7, 127.9, 129.0 (2C), 129.3, 131.0, 132.2, 139.2, 140.3, 144.7, 148.5, 151.6, 152.3, 166.3; MS (ESI) *m/z* 360.2 $[M+H]^+$; HRMS: calcd for $C_{20}H_{18}N_5O_2$ $[M+H]^+$ 360.1461, found 360.1455; HPLC t_R = 6.9 min, 98.9%.

2-(6-([1,1'-Biphenyl]-3-carboxamido)-9*H*-purin-9-yl)acetic acid (**12**): yield = 93 %; white powder; ^{1}H NMR (DMSO-d_6): δ = 5.16 (s, 2H), 7.44-7.72 (m, 4H), 7. 85 (d, 2H, ^3J = 7.2 Hz), 7.97-8.08 (m, 2H), 8.41 (s, 1H), 8.53 (s, 1H), 8.79 (s, 1H), 11.36 (bs, 1H); ^{13}C NMR (DMSO-d_6): δ = 45.3, 125.5, 127.6, 127.8 (2C), 128.5, 128.8, 129.9 (2C), 130.2, 131.5, 134.8, 140.2, 141.2, 146.1, 150.8, 152.5, 153.5, 166.4, 169.9; MS (ESI) *m/z* 374.1 $[M+H]^+$; HRMS: calcd for $C_{20}H_{16}N_5O_3$ $[M+H]^+$ 374.1253, found 374.1243; HPLC t_R = 7.1 min, 99.0%.

((6-([1,1'-Biphenyl]-3-carboxamido)-9H-purin-9-yl)methyl)phosphonic acid (**13**): To a stirred solution of compound **10** (0.32 mmol) in DMF (4.5 mL) at 0 °C was added under argon TMSBr (4.0 mmol). The solution was stirred at room temperature under argon for 48 h, then the reaction mixture was cooled to 0 °C and pH was adjusted to 7 with a solution of triethylammonium bicarbonate (TEAB) 1M. The mixture was concentrated under reduced pressure and the residue was successively purified by reverse phase (RP-18) chromatography (gradient: H_2O to MeOH) then silica gel chromatography using isocratic conditions ($IPrOH/NH_4OH/H_2O$, 7/2/1). Finally, a fraction of the compound was purified again by RP-18 chromatography (gradient: H_2O to MeOH) to provide compound **13** as a white powder (11%) and with sufficient purity; ^{1}H NMR (DMSO-d_6): δ = 4.48 (d, 2H, ^3J = 11.8 Hz), 7.44-7.71 (m, 4H), 7.84 (d, 2H, ^3J = 7.0 Hz), 7.95-8.05 (m, 2H), 8.39 (s, 1H), 8.50 (s, 1H), 8.77 (s, 1H), 11.36 (bs, 1H); ^{13}C NMR (DMSO-d_6): δ = 42.7 (d, ^1J = 133 Hz), 123.3, 126.8, 128.1, 128.4, 128.5, 129.8, 130.3 (2C), 133.1, 133.7, 140.2, 141.3, 146.0, 148.5, 151.3, 152.5, 162.1, 166.9; MS (ESI) *m/z* 410.2 $[M+H]^+$; HRMS: calcd for $C_{19}H_{17}N_5O_4P$ $[M+H]^+$ 410.1018, found 410.1012; HPLC t_R = 6.3 min, 97.8%.

(4-(3-Bromophenyl)-1H-imidazol-1-yl)methyl diethyl phosphate (15): To a stirred solution **14** [19] (4.48 mmol) in DMF (15 mL) was added under argon NaH 60% (8.21 mmol). After stirring at room temperature for 30 min, a solution of diethyl p-toluenesulfonyloxymethylphosphonate (2.5 eq.) in DMF (12.5 mL) was added over a 15 min period. The reaction mixture was stirred at 80 °C for 17 h. The volatiles were evaporated and the residue was purified on silica gel column chromatography (CH_2Cl_2/MeOH, 0-5%) to provide compound **15**.

yield = 86 %; ^{1}H NMR ($CDCl_3$): δ = 1.30 (t, J = 7.2 Hz, 6H), 4.11 (q, J = 6.9 Hz, 4H), 4.31 (d, 2H, ^3J = 12.3 Hz), 7.13-7.87 (m, 6H); ^{31}P NMR: 17.5. MS (ESI) *m/z* 749, 747, 745 $[2M+H]^+$; 375, 373 $[M+H]^+$

Ethyl 3'-(1-(((diethoxyphosphoryl)oxy)methyl)-1H-imidazol-4-yl)-[1,1'-biphenyl]-3-carboxylate (16): To a three-neck round-bottom flask under argon atmosphere was added $Pd(PPh_3)_4$ (0.1 eq.), DMF (27 mL) and compounds **15** (3.65 mmol). K_2CO_3 (3 eq.) and the corresponding 3-ethoxycarbonylbenzeneboronic acid (1.7 eq.) were successively added and the reaction mixture was stirred under argon at 100 °C until TLC revealed that the starting material was consumed. The mixture was cooled to room temperature, diluted with water and product was extracted with EtOAc. The organic layers were combined, dried over $MgSO_4$, concentrated *in vacuum* and the residue was purified by silica gel column chromatography (CH_2Cl_2/MeOH, 0-5%) to provide the desired compound **16**.

yield = 86%; ^{1}H NMR ($CDCl_3$): δ = 1.31 (t, J = 7.2 Hz, 6H), 1.42 (t, J = 7.2 Hz, 3H), 4.13 (q, J = 6.9 Hz, 4H), 4.34 (d, 2H, ^{3}J = 12.3 Hz), 4.40 (q, J = 6.9 Hz, 2H), 7.34-8.32 (m, 10H); ^{31}P NMR: 17.5. MS (ESI) *m/z* 885 $[2M+H]^+$; 443 $[M+H]^+$

3'-(1-((Ethoxy(hydroxy)phosphoryl)methyl)-1H-imidazol-4-yl)-[1,1'-biphenyl]-3-carboxylic acid (17*)*: To a stirred solution of compound **16** (1.38 mmol) in EtOH/dioxane (7.6 mL, 2:1, v:v) at 0 °C was added a solution of NaOH 2M (5 eq.). The solution was stirred at 80 °C until TLC revealed that the starting material was consumed. The reaction mixture was acidified until pH 2 with a solution of HCl 1N. The precipitate was filtered, washed with water, and dried to provide compound **17** as partially deprotected phosphonate.

yield = 76%; ^{1}H NMR (DMSO-d_6): δ = 1.19 (t, J = 9 Hz, 3H), 3.93 (q, J = 9 Hz, 2H), 4.40 (d, 2H, ^{3}J = 12 Hz), 7.45-7.95 (m, 8H), 8.19 (s, 1H), 8.37 (s, 1H); ^{31}P NMR: 12.1. MS (ESI) *m/z* 773 $[2M+H]^+$, 387 $[M+H]^+$

Synthesis of compounds (18) and (19) To a stirred solution of carboxylic acid **17** (1.42 mmol) in DMF (13 mL) was added under argon *N*,*N*'-carbonyldiimidazole (1.5 eq.), *N*,*N*-dimethyl-4-aminopyridine (0.2 eq.), adenine or **2a** (1.5 eq.). The reaction mixture was stirred at 100 °C until the starting material disappeared (checked by HPLC). Solvent was removed under reduced pressure and column chromatography of the crude materials on reverse phase (RP18, gradient: water to acetonitrile 100%) gave the expected ethylphosphonate which was passed through a Dowex Na^+ ion exchange column. The desired fractions were collected and freeze dried leading to the desired compounds **18** or **19** as sodium salt.

Sodium ethyl ((4-(3'-((7*H*-purin-6-yl)carbamoyl)-[1,1'-biphenyl]-3-yl)-1*H*-imidazol-1-yl) methyl) phosphonate (**18**): yield = 63%; ^{1}H NMR (DMSO-d_6): δ = 1.03 (t, J = 7 Hz, 3H), 3.65 (q, J = 7 Hz, 2H), 3.89 (d, J = 12 Hz, 2H), 7.40-8.47 (m, 10H), 8.53 (s, 1H), 8.75 (s, 1H), 11.80 (bs, 1H), 12.5 (bs, 1H); ^{13}C NMR (DMSO-d_6): δ = 16.9 (d, ^{3}J = 6 Hz), 44.7 (d, ^{1}J = 137 Hz), 59.2 (d, ^{2}J = 5.7 Hz), 117.5, 122.5, 123.7, 124.5, 126.0, 127.6, 129.2, 130.8, 135.8, 139.1, 139.5, 140.5, 146.1, 151.2, 166.5; ^{31}P NMR (DMSO-d_6): δ = 8.35; MS (ESI) *m/z* 504 $[M-Na+2H]^+$; HRMS: calcd for $C_{24}H_{23}N_7O_4P$ $[M-Na+2H]^+$ 504.1468, found 504.1549.

Sodium ethyl ((4-(3'-((7-((benzyloxy)methyl)-7H-purin-6-yl)carbamoyl)-[1,1'-biphenyl]-3-yl)-1*H*-imidazol-1-yl)methyl)phosphonate (19): yield = 6%; ^{1}H NMR (DMSO-d_6): δ = 1.03 (t, J = 7 Hz, 3H), 3.65 (q, J = 7 Hz, 2H), 3.91 (d, J = 12 Hz, 2H), 4.68 (s, 2H), 5.72 (s, 2H), 7.32-8.1 (m, 10H), 8.26 (s, 1H), 8.39 (s, 1H); ^{13}C NMR (DMSO-d_6): δ = 16.9, 44.7 (d, ^{1}J = 136 Hz), 59.2 (d, ^{2}J = 5.2 Hz), 70.9, 77.27, 117.4, 122.3, 123.1, 124.0, 124.2, 124.8, 127.1, 127.7, 128.1, 128.3, 129.1,

135.7, 137.5, 138.2, 139.1, 139.7, 140.2, 140.5, 142.6, 149.2, 150.4, 157.8, 173.2; ^{31}P NMR (DMSO-d_6): δ = 8.55; MS (ESI) *m/z* 623 [M-Na+2H]$^+$; HRMS: calcd for $C_{32}H_{31}N_7O_5P$ [M-Na+2H]$^+$ 624.2129, found 624.2124.

Sodium ((4-(3'-((7*H*-purin-6-yl)carbamoyl)-[1,1'-biphenyl]-3-yl)-1*H*-imidazol-1-yl) methyl) phosphonate (**20**)**:** The partially deprotected derivative **18** (1 eq.) was dissolved in anhydrous DMF (20 mL/mmol) and excess trimethylsilyl bromide (15-20 eq.) was added dropwise at 0 °C. The reaction mixture was stirred at room temperature until completion of the reaction was indicated by HPLC. Then, the reaction was stopped by adding triethylammonium bicarbonate buffer (TEAB 1 M, pH 7) and concentrated to dryness under high vacuum. Column chromatography of the crude materials on reverse phase (gradient: water to methanol 100%) gave the expected phosphonic acid (as triethylammonium salt), which was passed through a Dowex Na^+ ion exchange column. The desired fractions were collected and freeze dried leading to the title compounds **20** as sodium salt.
yield = 20%; ^{1}H NMR (D_2O): δ = 3.84 (d, J = 9 Hz, 2H), 6.82-7.5 (m, 10H), 8.0 (s, 1H), 8.2 (s, 1H); ^{13}C NMR (D_2O): δ = 46.9 (d, J = 137 Hz), 117.5, 121.4, 123.4, 124.6, 125.3, 126.8, 129.0, 129.3, 131.1, 131.7, 133.3, 138.4, 138.5, 139.8, 145.7, 150.7, 166.7; ^{31}P NMR (D_2O): δ = 10.7; MS (ESI) *m/z* 476.1 [M-Na+2H]$^+$; HPLC t_R = 5.2 min, 100%.

General procedure for Suzuki coupling reaction, Compounds **21a-e:** To a three-neck round-bottom flask under argon atmosphere was added $Pd(PPh_3)_4$ (0.14 mmol), DMF (9.5 mL) and commercially available 2-, 3- or 4-bromobenzonitrile (1.41 mmol). K_2CO_3 (4.24 mmol) and the corresponding 2-, 3- or 4-ethoxycarbonylbenzeneboronic acid (2.40 mmol) were successively added and the reaction mixture was stirred under argon at 100 °C until TLC revealed that the starting material was consumed. The mixture was cooled to room temperature, diluted with water and product was extracted with EtOAc. Organic layers were dried over $MgSO_4$, concentrated *in vacuum* and the residue was purified by silica gel column chromatography (petroleum ether/ EtOAc, 0-60%) to provide the desired compounds.

Ethyl 4'-cyano-[1,1'-biphenyl]-2-carboxylate (21a): yield = 74%; ^{1}H NMR ($CDCl_3$): δ 1.06 (t, 3H, J = 7.2 Hz), 4.12 (q, 2H, ^3J = 7.2 Hz), 7.30 (dd, ^3J = 7.5 Hz, ^4J = 0.9 Hz, 1H), 7.41 (d, ^3J = 8.4 Hz, 2H), 7.48 (td, ^3J = 7.5 Hz, ^4J = 1.5 Hz, 1H), 7.57 (td, ^3J = 7.5 Hz, ^4J = 1.5 Hz, 1H), 7.69 (d, ^3J = 8.1 Hz, 2H), 7.94 (dd, ^3J = 7.8 Hz, ^4J = 1.2 Hz 1H); MS (ESI+) 252.1 [M+H]$^+$, 224.1 [M-HCN], 206.1 [M-OEt]$^+$

Ethyl 3'-cyano-[1,1'-biphenyl]-3-carboxylate (21b): yield = 74%; ^{1}H NMR ($CDCl_3$): δ 1.34 (t, 3H, ^3J = 6.9 Hz), 4.33 (q, 2H, ^3J = 7.2 Hz), 7.47 (2t, ^3J = 7.5 Hz, 2H), 7.54-7.75 (3d, ^3J = 7.5 Hz,

3H), 7.80 (s, 1H), 7.99 (d, ^{3}J = 7.5 Hz, 1H), 8.14 (s, 1H); MS (ESI+) 252.1 $[M+H]^+$, 224.1 [M-HCN], 206.1 $[M-OEt]^+$

Ethyl 4'-cyano-[1,1'-biphenyl]-3-carboxylate (21c): yield = 71%; ^{1}H NMR ($CDCl_3$): δ 1.34 (t, 3H, ^{3}J = 6.9 Hz), 4.35 (q, 2H, ^{3}J = 7.2 Hz), 7.49 (t, J = 7.5 Hz, 1H), 7.66 (m, 5H), 8.02 (d, J = 7.8 Hz, 1H), 8.2 (s, 1H); MS (ESI+) 252.1 $[M+H]^+$, 224.1 [M-HCN]

Ethyl 2'-cyano-[1,1'-biphenyl]-4-carboxylate (21d): yield = 95%; ^{1}H NMR (DMSO-d_6): δ = 1.35 (t, J = 7.1 Hz, 3H), 4.35 (q, J = 7.1 Hz, 2H), 7.62-8.11 (m, 8H).; ^{1}H NMR ($CDCl_3$): δ = 1.42 (t, J = 7.1 Hz, 3H), 4.41 (q, J = 7.1 Hz, 2H), 7.49 (dd, ^{3}J = 7.5 Hz, ^{4}J = 0.9 Hz 1H), 7.53 (d, ^{3}J = 8.1 Hz, 1H), 7.63 (d, ^{3}J = 8.4 Hz, 2H), 7.68 (dd, ^{3}J = 7.5 Hz, ^{4}J = 0.9 Hz 1H), 7.79 (d, ^{3}J = 7.8 Hz, 1H), 8.16 (d, ^{3}J = 8.4 Hz, 2H); MS (ESI+) 252.1 $[M+H]^+$, 206.1 $[M-OEt]^+$

Ethyl 2'-cyano-[1,1'-biphenyl]-3-carboxylate (21e): yield = 92%; ^{1}H NMR (DMSO-d_6): δ = 1.35 (t, J = 7.1 Hz, 3H), 4.35 (q, J = 7.1 Hz, 2H), 7.61-8.12 (m, 8H). MS (ESI+) 252.1 $[M+H]^+$, 206.1 $[M-OEt]^+$

General procedure for synthesis of tetrazolo derivatives 22a-e: To a mixture of benzonitrile ester derivatives **21a-e** (0.453g, 1.8 mmol), sodium azide (0.351 g, 3eq.), and triethylamine hydrochloride (0.743 g, 3eq.) in NMP (18 ml) was heated at 150 °C for 20 h. The progress of the reaction was monitored by TLC (methanol: dichloromethane, 1:9, v:v). After completion, the reaction mixture was cooled to 0 °C, the pH was adjusted with concentrated HCl 3N. The solid precipitate was extracted with ethyl acetate twice. Again, it was washed with brine solution and dried over anhydrous sodium sulfate and evaporate to yield the product. The residue was purified by silica gel column chromatography (petroleum ether/ EtOAc, 10-60%) to provide the desired compounds.

Ethyl 4'-(2*H*-tetrazol-5-yl)-[1,1'-biphenyl]-2-carboxylate (22a): yield: 83%; ^{1}H NMR ($CDCl_3$): δ = 1.18 (t, ^{3}J = 6.9 Hz, 3H), 4.24 (q, ^{3}J = 6.9 Hz, 2H), 7.36 (dd, ^{3}J = 7.5 Hz, ^{4}J = 0.9 Hz 1H), 7.41 (d, ^{3}J = 8.4 Hz, 2H), 7.48 (td, ^{3}J = 7.5 Hz, ^{4}J = 1.5 Hz, 1H), 7.57 (td, ^{3}J = 7.5 Hz, ^{4}J = 1.5 Hz, 1H), 7.94 (dd, ^{3}J = 7.8 Hz, ^{4}J = 1.2 Hz, 1H), 7.98 (d, ^{3}J = 8.1 Hz, 2H); MS (ESI+) 883.3 $[3M+H]^+$, 589.2 $[2M+H]^+$, 295.1 $[M+H]^+$, MS (ESI-) 881.3 $[3M-H]^-$, 587.2 $[2M-H]^-$, 293.1 $[M-H]^-$

Ethyl 3'-(2*H*-tetrazol-5-yl)-[1,1'-biphenyl]-3-carboxylate (22b): yield: 74%; ^{1}H NMR (DMSO-d_6): δ = 1.42 (t, J = 7.2 Hz, 3H), 4.44 (q, J = 7.2 Hz, 2H), 7.73-8.18 (m, 6H), 8.35 (s, 1H), 8.43 (s, 1H). MS (ESI+) 589.2 $[2M+H]^+$, 295.1 $[M+H]^+$

Ethyl 2'-(2*H*-tetrazol-5-yl)-[1,1'-biphenyl]-3-carboxylate (22c): yield: 84%; ^{1}H NMR (DMSO-d_6): δ = 1.35 (t, J = 7.1 Hz, 3H), 4.36 (q, J = 7.1 Hz, 2H), 7.67 (t, J = 8 Hz, 1H), 7.96 (d, J = 8 Hz, 2H), 8.01 (d, J = 8 Hz, 1H), 8.05 (d, J = 8 Hz, 1H), 8.17 (d, J = 8 Hz, 2H), 8.27 (s, 1H); MS (ESI+) 589.2 $[2M+H]^+$, 295.1 $[M+H]^+$, MS (ESI-) 587.2 $[2M-H]^-$ 293.1 $[M-H]^-$, 265.1 $[M-Et]^-$

Ethyl 2'-(2*H*-tetrazol-5-yl)-[1,1'-biphenyl]-4-carboxylate (22d): yield: 75%; ^{1}H NMR (DMSO-d_6): δ = 1.32 (t, J = 7.1 Hz, 3H), 4.32 (q, J = 7.1 Hz, 2H), 7.24 (d, J = 8.1 Hz, 2H), 7.60 (d, J = 7.5 Hz, 2H), 7.65 (d, J = 7.3 Hz, 2H), 7.89 (d, J = 8.1 Hz, 2H). MS (ESI+) 295.1 $[M+H]^+$, 249.1 $[M-OEt]^+$ MS (ESI-) 293.1 $[M-H]^-$, 265.1 $[M-Et]^-$

Ethyl 2'-(2*H*-tetrazol-5-yl)-[1,1'-biphenyl]-3-carboxylate (22e): yield: 57%; ^{1}H NMR (DMSO-d_6): δ = 1.30 (t, J = 7.1 Hz, 3H), 4.29 (q, J = 7.1 Hz, 2H), 7.33-7.91 (m, 8H). MS (ESI+) 295.1 $[M+H]^+$, 249.1 $[M-OEt]^+$ MS (ESI-) 293.1 $[M-H]^-$, 265.1 $[M-Et]^-$

General procedure for saponification of methyl ester derivatives, compounds 23a-e. To a stirred solution of compound **22a-e** (4.82 mmol) in a mixture of EtOH and dioxane (33 mL, 2:3, v:v) at 0 °C was added a solution of NaOH 2M (5 eq.). The solution was stirred at 60-80 °C until TLC revealed that the starting material has disappeared. The reaction mixture was acidified until pH 2 with a solution of HCl 2N. The precipitate was filtered, extracted with ethyl acetate and dried over anhydrous magnesium sulfate to provide carboxylic acid derivatives **23a-e** in nearly quantitative yields (90 to 100%). All compounds were considered pure enough (as determined by HPLC) to be used without further purification.

General procedure for synthesis of compounds 24a-e and 25. To a stirred solution of carboxylic acid **23a-e** (400 mg, 1.5 mmol) in DMF (15 mL) was added under argon *N*,*N*'-carbonyldiimidazole (1.5 eq.), *N*,*N*-dimethyl-4-aminopyridine (0.2 eq.), adenine or *N*-9 substituted adenine **4** (3 eq.). The reaction mixture was stirred at 100 °C until HPLC revealed that the starting material was consumed. Volatiles were removed under reduced pressure. Excess of adenine was precipitated in isopropanol, filtered off and the filtrate was evaporated. The residue was firstly purified by silica gel column chromatography (CH_2Cl_2/EtOH/AcOH,90/5/5, v/v/v) and then on reverse phase (RP18 using a gradient of water to methanol containing 1% AcOH) to provide the desired compounds.

***N*-(9*H*-Purin-6-yl)-4'-(2*H*-tetrazol-5-yl)-[1,1'-biphenyl]-2-carboxamide (24a):** yield = 15%; ^{1}H NMR (DMSO-d_6): δ = 7.07-8.09 (m, 9H), 8.40 (s, 1H), 8.57 (s, 1H), 11.49 (bs, 1H) ^{13}C NMR (DMSO-d_6): δ = 126.5, 127.7, 129.2, 130.2, 130.5, 131.2, 135.4, 139.8, 140.2, 146.4, 151.6, 152.9, 159.5, 169.8 MS (ESI-) *m/z* 765.2 $[2M-H]^-$, 382.1 $[M-H]^-$, MS (ESI+) 767.3 $[2M+H]^+$ 384.1 $[M+H]^+$; HRMS: calcd for $C_{19}H_{14}N_9O$ $[M+H]^+$ 384.1321, found 384.1324; HPLC t_R = 9.16 min, 100%.

***N*-(9*H*-Purin-6-yl)-3'-(2*H*-tetrazol-5-yl)-[1,1'-biphenyl]-3-carboxamide (24b):** yield = 45%; ^{1}H NMR (DMSO-d_6): δ = 6.92-8.12 (m, 7H), 8.47 (s, 1H), 8.51 (s, 1H), 8.75 (s, 1H), 11.78 (bs, 1H) ^{13}C NMR (DMSO-d_6): δ = 107.0, 124.7, 125.8, 126.9, 127.0, 127.8, 129.4, 129.6, 130.4, 130.9, 133.6,

139.7, 140.1, 145.9, 151.2, 152.5, 158.8, 166.5 MS (ESI-) *m/z* 765.2 $[2M-H]^-$, 382.1 $[M-H]^-$, MS (ESI+) 384.1 $[M+H]^+$; HRMS: calcd for $C_{19}H_{14}N_9O$ $[M+H]^+$ 384.1321, found 384.1318; HPLC t_R = 10.5 min, 96.4 %

***N*-(9*H*-Purin-6-yl)-4'-(2*H*-tetrazol-5-yl)-[1,1'-biphenyl]-3-carboxamide (24c):** yield = 53%; ^{1}H NMR (DMSO-d_6): δ = 6.95-8.19 (m, 7H), 8.52 (s, 1H), 8.55 (s, 1H), 8.76 (s, 1H); 11.78 (bs, 1H); ^{13}C NMR (DMSO-d_6): δ = 107.0, 125.5, 126.8, 127.3, 127.7, 128.2, 129.4, 130.9, 133.6, 139.3, 139.4, 140.1, 145.9, 151.2, 152.4, 156.3, 166.3 MS (ESI-) *m/z* 382.1 $[M-H]^-$, MS (ESI+) 384.1 $[M+H]^+$; HRMS: calcd for $C_{19}H_{14}N_9O$ $[M+H]^+$ 384.1321, found 384.1327; HPLC t_R = 9.6 min, 96.5%.

***N*-(9*H*-Purin-6-yl)-2'-(2*H*-tetrazol-5-yl)-[1,1'-biphenyl]-4-carboxamide (24d):** yield = 17%; ^{1}H NMR (DMSO-d_6): δ = 7.27-8.06 (m, 8H), 8.49 (s, 1H), 8.72 (s, 1H), 11.54 (bs, 1H); 12.39 (bs, 1H); ^{13}C NMR (DMSO-d_6): δ = 124.4, 128.9, 129.0, 129.4, 131.1, 131.5, 132.1, 140.9, 144.2, 146.5, 151.6, 155.8, 166.5, MS (ESI-) *m/z* 1148.4 $[3M-H]^-$, 765.2 $[2M-H]^-$, 382.1 $[M-H]^-$, MS (ESI+) 767.3 $[2M+H]^+$ 384.1 $[M+H]^+$; HRMS: calcd for $C_{19}H_{14}N_9O$ $[M+H]^+$ 384.1321, found 384.1327; HPLC t_R = 9.26 min, 100%.

***N*-(9*H*-Purin-6-yl)-2'-(2*H*-tetrazol-5-yl)-[1,1'-biphenyl]-3-carboxamide (24e)** yield = 56%; ^{1}H NMR (DMSO-d_6): δ = 7.20-8.08 (m, 8H), 8.48 (s, 1H), 8.71 (s, 1H), 11.55 (bs, 1H); 12.37 (bs, 1H); ^{13}C NMR (DMSO-d_6): δ = 124.4, 128.1, 128.7, 128.8, 129.5, 129.6, 131.0, 131.4, 133.4, 140.2, 141.0, 146.4, 151.6, 155.9, 166.7, MS (ESI-) *m/z* 1148.4 $[3M-H]^-$, 765.2 $[2M-H]^-$, 382.1 $[M-H]^-$, MS (ESI+) 767.3 $[2M+H]^+$ 384.1 $[M+H]^+$; HRMS: calcd for $C_{19}H_{14}N_9O$ $[M+H]^+$ 384.1321, found 384.1320; HPLC t_R = 9.24 min, 100%.

Ethyl 2-(6-(2'-(2*H*-tetrazol-5-yl)-[1,1'-biphenyl]-4-carboxamido)-9*H*-purin-9-yl)acetate (25): yield = 15%; ^{1}H NMR (DMSO-d_6): δ = 1.24 (t, 3H, ^3J = 7.0 Hz), 4.21 (q, 2H, ^3J = 7.0 Hz), 5.25 (s, 2H), 7.27-7.98 (m, 8H), 8.48 (s, 1H), 8.74 (s, 1H), 11.24 (bs, 1H); ^{13}C NMR (DMSO-d_6): δ = 14.5, 44.8, 62.0, 125.4, 128.4, 128.5, 128.6, 129.5, 129.8, 130.8, 131.0, 132.1, 140.4, 141.2, 145.3, 150.7, 152.1, 158.3, 165.9, 168.2; MS (ESI-) *m/z* 1406.5 $[3M-H]^-$, 937.3 $[2M-H]^-$, 468.15 $[M-H]^-$, MS (ESI+) 939.3 $[2M+H]^+$ 470.2 $[M+H]^+$; HRMS: calcd for $C_{23}H_{20}N_9O_3$ $[M+H]^+$ 470.1692, found 470.1689; HPLC t_R = 9.49 min, 96.6%.

ASSOCIATED CONTENT

Supporting Information. The following files are available free of charge: Additional figures and tables illustrating content of the various flasks used during library generation, inhibition and structural (file type, i.e., word document). Spectral data of final compounds and few intermediates including NMR and MS spectra (file type, PDF).

AUTHOR INFORMATION

Corresponding Authors

Dr S. PEYROTTES, email: suzanne.peyrottes@umontpellier.fr , Tel: +33 (0)4 67 14 49 64

ORCID: 0000-0003-1705-0576

Dr Laurent CHALOIN, email: laurent.chaloin@irim.cnrs.fr , Tel: +33 (0)4 34 35 94 66

ORCID: 0000-0002-5757-5804

Author Contributions

The manuscript was written with contributions of all authors. All authors have given approval to the final version of the manuscript.

ACKNOWLEDGMENTS

This work was supported by Institutional funds from the Institut National du Cancer (INCa, project n°2010-200 "Nucleotarg") and the Agence Nationale de la Recherche (ANR Programme Blanc 2011-SIMI7, "cN-II Focus"). We thank E. Cros-Perrial, F. Galisson, C. Rabeson and J. Gobbi for excellent technical assistance. Technical support from staff on MX beamlines (European Synchrotron Radiation Facility Grenoble France) and the Swiss Light Source (Villigen Switzerland) is gratefully acknowledged. We are also grateful for assistance from V. Gueguen-Chaignon and I. Zanella-Cléon of the Protein Science Facility of SFR Biosciences Lyon (UMS3444/US8). R. Rahimova was supported by a fellowship from the Ligue contre le cancer. We kindly thank Dr Corinne Lionne for helpful discussions and Mrs M.C. Bergogne for manuscript edition.

ABBREVIATIONS

AMP, adenosine 5'-monophosphate; BOM, benzyloxymethyl; CCRF-CEM, human acute lymphoblastic leukemia cells; CD73, 5'-ectonucleotidase; CDI, *N*,*N'*-carbonyldiimidazole; cdN, cytosolic 3',5'-deoxy-nucleotidase; cN-I, cN-II, or cN-III , cytosolic 5'-nucleotidase I, II or III; DMAP, 4-dimethylaminopyridine; DMF, *N*,*N*-dimethylformamide; DMSO, dimethyl sulfoxide; FBDD, fragment-based drug discovery; HL-60, human acute promyelocytic leukemia cells; HPLC, high performance liquid chromatography; IMP, inosine 5'-monophosphate; mdN, mitochondrial nucleotidase; MTT, 3-(4,5-dimethylthiazol-2-yl)-2,5-diphenyl tetrazolium bromide; NMP, *N*-methyl-2-pyrrolidone; NMR, nuclear magnetic resonance; RL, human follicular lymphoma cells; rt, room temperature; shRNA, short hairpin ribonucleic acid; TMSBr, trimethylsilyl bromine; UV, Ultra-violet.

Protein Data Bank (http://www.rcsb.org) entry codes: 6FIR (cN-II-2132, 5 mM), 6FXH (cN-II-2132, 10 mM), 6FIS (cN-II-**2a**), 6FIW (cN-II-**20**) and 6FIU (cN-II-**12**). Authors will release the atomic coordinates and experimental data upon article publication.

REFERENCES

1. Bianchi, V. and J. Spychala, *Mammalian 5 '-nucleotidases.* Journal of Biological Chemistry, 2003. **278**(47): p. 46195-46198.
2. Hunsucker, S.A., B.S. Mitchell, and J. Spychala, *The 5'-nucleotidases as regulators of nucleotide and drug metabolism.* Pharmacology & Therapeutics, 2005. **107**(1): p. 1-30.
3. Buschmann, J., et al., *Identification of Drosophila and human 7-methyl GMP-specific nucleotidases.* The Journal of biological chemistry, 2013. **288**(4): p. 2441-2451.
4. Zanella, A., et al., *Hereditary pyrimidine 5 '-nucleotidase deficiency: from genetics to clinical manifestations.* British Journal of Haematology, 2006. **133**(2): p. 113-123.
5. St Hilaire, C., et al., *NT5E Mutations and Arterial Calcifications.* New England Journal of Medicine, 2011. **364**(5): p. 432-442.
6. Dursun, U., et al., *Autosomal recessive spastic paraplegia (SPG45) with mental retardation maps to 10q24.3-q25.1.* Neurogenetics, 2009. **10**(4): p. 325-331.
7. Guan, F.L., et al., *Two-stage replication of previous genome-wide association studies of AS3MT-CNNM2-NT5C2 gene cluster region in a large schizophrenia casecontrol sample from Han Chinese population.* Schizophrenia Research, 2016. **176**(2-3): p. 125-130.
8. Novarino, G., et al., *Exome Sequencing Links Corticospinal Motor Neuron Disease to Common Neurodegenerative Disorders.* Science, 2014. **343**(6170): p. 506-511.
9. Jordheim, L.P. and L. Chaloin, *Therapeutic Perspectives for cN-II in Cancer.* Current Medicinal Chemistry, 2013. **20**(34): p. 4292-4303.
10. Meyer, J.A., et al., *Relapse-specific mutations in NT5C2 in childhood acute lymphoblastic leukemia.* Nature Genetics, 2013. **45**(3): p. 290-294.
11. Tzoneva, G., et al., *Activating mutations in the NT5C2 nucleotidase gene drive chemotherapy resistance in relapsed ALL.* Nature Medicine, 2013. **19**(3): p. 368-371.
12. Jordheim, L., et al., *Determination of the enzymatic activity of cytosolic 5'-nucleotidase cN-II in cancer cells: development of a simple analytical method and related cell line models.* Analytical and Bioanalytical Chemistry, 2015. **407**(19): p. 5747-5758.
13. Skladanowski, A.C., G.B. Sala, and A.C. Newby, *Inhibition of IMP-specific cytosolic 5'-nucleotidase and adenosine formation in rat polymorphonuclear leucocytes by 5'-deoxy-5'-isobutylthio derivatives of adenosine and inosine.* Biochemical Journal, 1989. **262**(1): p. 203-208.
14. Cividini, F., et al., *The purine analog fludarabine acts as a cytosolic 5'-nucleotidase II inhibitor.* Biochemical Pharmacology, 2015. **94**(2): p. 63-68.
15. Jordheim, L.P., et al., *Identification and characterization of inhibitors of cytoplasmic 5 '-nucleotidase cN-II issued from virtual screening.* Biochemical Pharmacology, 2013. **85**(4): p. 497-506.
16. Gallier, F., et al., *Structural Insights into the Inhibition of Cytosolic 5'-Nucleotidase II (cN-II) by Ribonucleoside 5'-Monophosphate Analogues.* PLoS Comput Biol, 2011. **7**(12): p. e1002295.
17. Meurillon, M., et al., *Structure–activity relationships of β-hydroxyphosphonate nucleoside analogues as cytosolic 5'-nucleotidase II potential inhibitors: Synthesis, in vitro evaluation*

and molecular modeling studies. European Journal of Medicinal Chemistry, 2014. **77**(0): p. 18-37.
18. Nguyen Van, T., et al., *Beta-hydroxyphosphonate ribonucleoside analogues derived from 4-substituted-1,2,3-triazoles as IMP/GMP mimics: synthesis and biological evaluation.* Beilstein Journal of Organic Chemistry, 2016. **12**: p. 1476-1486.
19. Marton, Z., et al., *Identification of Noncompetitive Inhibitors of Cytosolic 5'-Nucleotidase II Using a Fragment-Based Approach.* Journal of medicinal chemistry, 2015. **58**(24): p. 9680-96.
20. Bretonnet, A.S., et al., *NMR screening applied to the fragment-based generation of inhibitors of creatine kinase exploiting a new interaction proximate to the ATP binding site.* Journal of Medicinal Chemistry, 2007. **50**(8): p. 1865-1875.
21. Hage-Melim, L.I.D., et al., *Computer-aided Drug Design of Novel PLA(2) Inhibitor Candidates for Treatment of Snakebite.* Journal of Biomolecular Structure & Dynamics, 2009. **27**(1): p. 27-35.
22. Wallden, K., et al., *Crystal structure of human cytosolic 5 '-nucleotidase II - Insights into allosteric regulation and substrate recognition.* Journal of Biological Chemistry, 2007. **282**(24): p. 17828-17836.
23. Krovat, E.M., K.H. Fruhwirth, and T. Langer, *Pharmacophore identification, in silico screening, and virtual library design for inhibitors of the human factor Xa.* Journal of Chemical Information and Modeling, 2005. **45**(1): p. 146-159.
24. Prasad, C.V.S.S., K.K. Chaudhary, and P. Dinkar, *A Combinatorial approach: To design inhibitory molecules on Hemagglutinin protein of H1N1 virus (Swine Flu).* Bioinformation, 2013. **9**(11): p. 565-571.
25. Wallden, K. and P. Nordlund, *Structural Basis for the Allosteric Regulation and Substrate Recognition of Human Cytosolic 5 '-Nucleotidase II.* Journal of Molecular Biology, 2011. **408**(4): p. 684-696.
26. Hakimelahi, G.H., et al., *Design, synthesis, and biological evaluation of novel nucleoside and nucleotide analogues as agents against DNA viruses and/or retroviruses.* Journal of Medicinal Chemistry, 2001. **44**(22): p. 3710-3720.
27. Prekupec, S., et al., *Synthesis and comparative cytostatic activity of the new N-7 acyclic purine nucleoside analogues with natural N-9 regioisomers.* Heterocycles, 2005. **65**(4): p. 787-796.
28. Bronson, J.J., et al., *A new synthesis of the potent and selective anti-herpes virus agent (S)-1-3-hydroxy-2-(phosphonylmethoxy)propyl cytosine.* Nucleosides & Nucleotides, 1990. **9**(6): p. 745-769.
29. Chou, T.-C. and P. Talalay, *Quantitative analysis of dose-effect relationships: the combined effects of multiple drugs or enzyme inhibitors.* Advances in Enzyme Regulation, 1984. **22**: p. 27-55.
30. Pedretti, A., L. Villa, and G. Vistoli, *VEGA - An open platform to develop chemo-bio-informatics applications, using plug-in architecture and script programming.* Journal of Computer-Aided Molecular Design, 2004. **18**(3): p. 167-173.
31. Gasteiger, J. and M. Marsili, *Iterative partial equalization of orbital electronegativity - A rapid access to atomic charges.* Tetrahedron, 1980. **36**(22): p. 3219-3228.
32. Jones, G., P. Willett, and R.C. Glen, *Molecular recognition of receptor-sites using a genetic algorithm with a description of desolvation.* Journal of Molecular Biology, 1995. **245**(1): p. 43-53.
33. Jones, G., et al., *Development and validation of a genetic algorithm for flexible docking.* Journal of Molecular Biology, 1997. **267**(3): p. 727-748.

34. Wallden, K., et al., *Crystal structures of human and murine deoxyribonucleotidases: Insights into recognition of substrates and nucleotide analogues.* Biochemistry, 2007. **46**(48): p. 13809-13818.
35. Kabsch, W., *XDS.* Acta Crystallographica Section D-Biological Crystallography, 2010. **66**: p. 125-132.
36. McCoy, A.J., et al., *Phaser crystallographic software.* Journal of Applied Crystallography, 2007. **40**: p. 658-674.
37. Adams, P.D., et al., *PHENIX: a comprehensive Python-based system for macromolecular structure solution.* Acta Crystallographica Section D-Biological Crystallography, 2010. **66**: p. 213-221.
38. Murshudov, G.N., et al., *REFMAC5 for the refinement of macromolecular crystal structures.* Acta Crystallographica Section D-Biological Crystallography, 2011. **67**: p. 355-367.
39. Emsley, P. and K. Cowtan, *Coot: model-building tools for molecular graphics.* Acta Crystallographica Section D-Biological Crystallography, 2004. **60**: p. 2126-2132.
40. Schuttelkopf, A.W. and D.M.F. van Aalten, *PRODRG: a tool for high-throughput crystallography of protein-ligand complexes.* Acta Crystallographica Section D-Biological Crystallography, 2004. **60**: p. 1355-1363.
41. Winn, M.D., et al., *Overview of the CCP4 suite and current developments.* Acta Crystallographica Section D-Biological Crystallography, 2011. **67**: p. 235-242.
42. Zhang, Y. and J. Skolnick, *Scoring function for automated assessment of protein structure template quality.* Proteins-Structure Function and Bioinformatics, 2004. **57**(4): p. 702-710.
43. Bliman, D., et al., *8-Bromination of 2,6,9-trisubstituted purines with pyridinium tribromide.* Tetrahedron Letters, 2014. **55**(18): p. 2929-2931.
44. Petrov, V.I., et al., *9-(2-Aryloxyethyl) Derivatives of Adenine - a New Class of Non-nucleosidic Antiviral Agents.* Chemistry of Heterocyclic Compounds, 2003. **39**(9): p. 1218-1226.
45. Zhang, L., et al., *7'-Substituted Benzothiazolothio- and Pyridinothiazolothio-Purines as Potent Heat Shock Protein 90 Inhibitors.* Journal of Medicinal Chemistry, 2006. **49**(17): p. 5352-5362.
46. Skwarczynski, M., et al., *Thymine, adenine and lipoamino acid based gene delivery systems.* Chemical Communications, 2010. **46**(18): p. 3140-3142.